

B  
Posted  
add

**GEORGIA INSTITUTE OF TECHNOLOGY**  
OFFICE OF RESEARCH ADMINISTRATION

**RESEARCH PROJECT INITIATION**

Date: June 7, 1974

Project Title: **Research Initiation - Resonant Frequencies and Natural Modes of Arbitrarily Shaped Ducts.**

Project No: **E-16-647**

Principal Investigator **Dr. William A. Bell**

Sponsor: **National Science Foundation**

Agreement Period: From **April 1, 1974** Until **March 31, 1976\***  
**\*18 month budget period plus 6 months for submission of required reports, etc.**

Type Agreement: **Grant GK-42159**

Amount: **\$17,000 - NSF Funds (E-16-647)**  
**3,432 - GIT Contrib. (E-16-342)**  
**\$20,432 - Total**

Reports Required: **Annual Letter Technical; Final Report**

Sponsor Contact Person (s):

**Administrative Matters**  
**Mr. F. G. Naughten**  
**Grants Manager, Area 4**  
**National Science Foundation**  
**Washington, D. C. 20550**  
**Phone: (202) 632-5965**

**Technical Matters**  
**Dr. Michael P. Gaus, Head**  
**Engineering Mechanics Section**  
**Industrial Technology Program**  
**National Science Foundation**  
**Washington, D. C. 20550**  
**Phone: (202) 632-5787**

Assigned to: **School of Aerospace Engineering**

**COPIES TO:**

Principal Investigator	Library
School Director	Rich Electronic Computer Center
Dean of the College	Photographic Laboratory
Director, Research Administration	Project File
Director, Financial Affairs (2)	
Security-Reports-Property Office	
Patent Coordinator	Other _____

SPONSORED PROJECT TERMINATION

Date: April 19, 1976

Project Title: Research Initiation - Resonant Frequencies and Natural Modes of Arbitrarily Shaped Ducts

Project No: E-16-647

Project Director: Dr. William A. Bell

Sponsor: National Science Foundation

Effective Termination Date: March 31, 1976

Clearance of Accounting Charges: 3/31/76

Grant/Contract Closeout Actions Remaining:

- ☐ Final Invoice and Closing Documents
- ☒ Final Fiscal Report
- ☐ Final Report of Inventions
- ☐ Govt. Property Inventory & Related Certificate
- ☐ Classified Material Certificate
- ☐ Other \_\_\_\_\_

Assigned to: Aerospace Engineering (School/Laboratory)

COPIES TO:

Project Director  
Division Chief (EES)  
School/Laboratory Director  
Dean/Director-EES  
Accounting Office  
Procurement Office  
Security Coordinator (OCA) ✓  
Reports Coordinator (OCA)

Library, Technical Reports Section  
Office of Computing Services  
Director, Physical Plant  
EES Information Office  
Project File (OCA)  
Project Code (GTRI)  
Other \_\_\_\_\_

NSF Grant -  
No Property Actions  
OAH

NATIONAL SCIENCE FOUNDATION GRANT GK-42159  
GEORGIA TECH CONTRACT NUMBER E-16-647

Research Initiation

RESONANT FREQUENCIES AND NATURAL MODES  
OF ARBITRARILY SHAPED DUCTS

ANNUAL REPORT FOR THE PERIOD APRIL 1, 1974 TO APRIL 1, 1975

PREPARED BY:

WILLIAM A. BELL  
PRINCIPAL INVESTIGATOR

School of Aerospace Engineering  
Georgia Institute of Technology  
Atlanta, Georgia 30332

## I. INTRODUCTION

### A. Program Objectives

The objective of this research grant is the development of a general analytical technique for the prediction of the resonant frequencies and natural modes of acoustic waves inside arbitrarily shaped ducts with mixed boundary conditions. Such a technique is needed to predict and improve the acoustic properties of systems used in domestic and industrial applications. To achieve this objective, an integral formulation of the wave equation is used because of computational advantages. To evaluate the accuracy of the numerical technique, it is applied to ducts with simple geometries and boundary conditions for which exact solutions exist. The numerical results are then compared with the exact solutions. For more complicated shapes and boundary conditions for which no exact analysis exists, the predicted results are to be compared with experimental data or published numerical values obtained by other analytical techniques.

### B. Background

In this study, the problem is to solve the two-dimensional Helmholtz equation - shown in Figure 1(A) - for a given geometry and boundary condition. This equation describes the spatial dependence of harmonic oscillations in a frictionless, homogeneous, perfect gas. This equation also describes the propagation of electromagnetic waves so that the techniques for obtaining a solution for the acoustic problem can be applied directly to electromagnetic wave propagation. Modified forms of the Helmholtz equation are also used in the fields of heat conduction, potential theory, and aeroelasticity.



To determine the resonant frequencies and natural modes of wave guides, the differential formulation is currently the most widely used. In differential form, exact solutions of the Helmholtz equation can be obtained by separation of variables. The eigenvalues and wave shapes are dependent upon the boundary conditions for a given geometry. The main limitation of this technique in the present study is that it is restricted to special coordinate systems and boundary conditions for which the separation of variables can be applied. Therefore, this technique cannot be used in the general problem of concern in this research grant.

For arbitrarily shaped bodies, the differential form of the Helmholtz equation can be solved by writing the equation in terms of finite differences. The resulting matrix of algebraic equations are then solved for the acoustic potential at every point within the duct. Once the potential values are known, the acoustic pressure and velocity can then be determined. To obtain sufficient accuracy, fine grid sizes must be used which necessitate large computer storage and computation times for the matrix of equations. Because of the storage requirements and the computer time involved in solving the matrix, the method has only been applied to two-dimensional problems.

Since a numerical technique must usually be employed to solve the governing equations for wave propagation inside arbitrarily shaped surfaces, the integral form of the Helmholtz equation is employed because it is more suitable for numerical solution. The integral form is obtained by applying Green's theorem to the differential equation. As shown by equation (B) in Figure 1, this formulation relates the value of the acoustic potential function at any point P inside the surface to the values of the

function at the surface. Unlike the differential Helmholtz equation which involves the simultaneous determination of the acoustic field at every point in the interior domain, the integral formulation reduces the problem to the much simpler one of determining the wave form at the surface by solving equation (C) in Figure 1. Essentially the number of dimensions of the problem is reduced by one. Thus, the computer storage required for numerically solving the integral form of the Helmholtz equation is much less than the storage requirements and associated computation times necessary for obtaining solutions by finite differences.

#### C. Summary of the Work Conducted to Date

This study can be divided into two parts. The first part is the development of numerical techniques for computing the eigenmodes and eigenvalues from the integral equations. These methods are discussed in Section II. The second part consists of the application of the equations to specific geometries. The geometries investigated to date are presented in Section III and include the study of a right circular cylinder, a rectangle, and a star-shaped boundary. For rigid walls, where the normal derivative of the potential is zero at the surface, exact and computed results compare to three decimal places for the cases considered. For an admittance condition at the boundary, the exact and computed eigenvalues compare to within two per cent. The further tasks which will be performed to complete the requirements of this grant are presented in Section IV along with proposed future studies.

## II. SOLUTION TECHNIQUE

The solution technique consists of (1) discretization of the integral

equations in Figure 1, (2) specification of the surface geometry and boundary conditions, and (3) determination of the eigenmodes and eigenvalues.

#### A. Discretization of the Integral Equation

Applying the trapezoidal rule to the integral equation for the surface potential gives the discretized equation, presented in Figure 2. The admittance condition is used to relate the potential to its normal derivative at the surface. The discretized equation is used to generate a system of complex, linear, homogeneous, algebraic equations to be solved for the potential at discrete points on the surface. To obtain a non-trivial solution the determinant of the coefficient matrix must be zero. The values of  $k$  for which this determinant is zero are the eigenvalues or resonant frequencies of the duct.

#### B. Surface Geometry and Boundary Conditions

To determine the coefficients of the potential for the discretized integral equation, the geometry must first be specified so that the distances  $r_{im}$  and the normal derivatives can be obtained. Once computed, the Hankel functions,  $H_0^{(1)}$  and  $H_1^{(1)}$ , can then be determined for a given value of  $k$ .

In the study conducted under this research grant, a computer program has been written which evaluates the distances and normal derivatives for a given geometry and integration stepsize  $s_i$ . The geometry can be specified either by parametric equations or, in the more general case, by inputting the coordinates and normal derivatives at each point on the boundary. Techniques applicable to all but the most general shapes have been

developed for taking advantage of the symmetry of the surface to minimize computation time and storage requirements. For instance, for the circular boundary considered in this study, only one set of coefficients between a boundary point at  $M$  and the other  $i$  boundary points need be computed for a constant surface admittance and integration stepsize. As shown in Figure 3, once the distances  $r_{im}$  and normal derivatives have been obtained at  $m$ , they can be used at another boundary point  $M + N$  by keeping track of the relative location of  $M + N$  with respect to  $M$ . Similar simplifications have been used for the rectangular and star shapes considered in this study. Special considerations have also been included for handling boundaries with corners, at which the normal derivative is undefined. Although it was proposed to consider boundaries with a uniform surface admittance only, the computer program is capable of handling admittance values which vary over the boundary.

### C. Determination of the Resonant Frequencies and Natural Mode Shapes

Once the coefficients of the surface potentials at each discrete point on the surface have been determined, the values of the nondimensional frequency  $k$  for which the determinant of the coefficient matrix is zero can be found. These values of  $k$  correspond to the resonant frequencies or eigenvalues of the duct under consideration.

Because  $k$  appears both as a multiplicative factor and as part of the argument of the Hankel function as shown in Figure 2, the problem is a nonlinear matrix eigenvalue problem. Thus, the numerical techniques available to solve for a linear matrix eigenvalue cannot guarantee convergence.

This problem is resolved in the present study by employing a quadratic



interpolation algorithm. This algorithm is rapidly convergent and is capable of computing complex zeroes for complicated functions which cannot be written explicitly. To find an eigenvalue three starting values must be assumed. For the case of a rigid wall, the eigenvalues are real numbers, so successive real values of  $k$  are assumed until the magnitude of the coefficient matrix determinant reaches a minimum. The determinant is computed using a complex Gauss-Jordan elimination technique. This minimum value of  $k$  along with the preceding and succeeding values are then used as the three starting points in the quadratic interpolation scheme. A typical plot of the magnitude of the determinant of the coefficient matrix versus  $k$  is given in Figure 4 for the star-shaped geometry. The values at which the determinant is minimized correspond to the natural frequencies. For a complex admittance condition at the boundary, the search vector for  $k$  is taken along the line  $-Y_j + iY_j$  in the complex plane using the rigid wall resonant frequency as the starting point.

This solution technique has been used successfully to determine the eigenfrequencies of the circle, rectangle, and star. Computation times for determining an eigenfrequency on the grantee-owned U1108 range from ten seconds for the circle to sixty seconds for the rectangle and star.

To determine the resonant mode shape at a given eigenfrequency, the equations are normalized with respect to one of the surface potentials and reduced using a Gauss-Jordan matrix reduction scheme for complex coefficients. The interior points can then be found by employing the discretized form of equation (C) in Figure 1. To compute the mode shapes, from five to sixty seconds of computation time are required for nine to fifty-two

interior points, respectively. In these calculations, techniques for taking advantage of symmetry have been developed to reduce time and storage requirements.

### III. RESULTS

Using the numerical techniques described in the last sections, solutions have been obtained for the resonant frequencies and natural modes of a circle, rectangle, and star. To demonstrate the accuracy of the numerical technique, the approximate results obtained in this study for the circle and rectangle are compared with exact computations.

#### A. Circle

For a circle, these comparisons are presented in Table I. In this table the numerical and exact eigenfrequencies are tabulated for three admittance values -  $y = 0$ ,  $y = .3i$ , and  $y = .3$  - for thirty points on the boundary. The best agreement between the computed and exact results occurs at the zero admittance condition. The real part of the eigenfrequencies compare to almost five significant figures and the imaginary parts are accurate to .001 for the first five modes. When a nonzero admittance condition is introduced, the accuracy is reduced to two significant figures in the real part and to .02 in the imaginary part of the eigenfrequencies.

The accuracy of the computed natural mode shapes follows the same trend. As shown in Figure 5, the agreement between the exact and computed eigenmodes for a rigid boundary is to within .01 per cent for interior points sufficiently far removed from the boundary. For a nonzero admittance at the surface, the accuracy is to within two per cent as presented in Figure 6.

This discrepancy in the accuracies obtained for the rigid and nonrigid

boundaries has been the subject of a recent investigation conducted under this grant. For a nonzero admittance, the source of this discrepancy was traced to the appearance of the zeroth order Hankel function which has a logarithmic singularity as the distance between two boundary points goes to zero. Unlike the first order Hankel function which has a  $1/r$ -type singularity, the logarithmic singularity of  $H_0^{(1)}$  has not been removed analytically. To resolve this problem, a Gaussian integration for a logarithmic singularity is used around the singular point and the standard Gauss-Legendre integration is used to obtain the coefficients at the other points. Preliminary results are shown in Table I for  $y = 0.3$ . The use of the Gaussian integration formulas appears to increase the accuracy of the numerical results by two orders of magnitude. Thus far the Gaussian formulas have only been applied to the circle. They will also be employed with the other shapes to increase the accuracy of the results since their use involves only about a one per cent increase in computer time.

Another problem which is under investigation is the deterioration of accuracy for interior points close to the boundary. This phenomenon occurs because of the proximity of the interior point to the jump condition at the boundary. Both analytical and numerical approaches for avoiding this problem are currently under scrutiny.

## B. Rectangle

The main reason for studying the rectangle is to investigate methods for handling corner points. At these points the normal derivatives are undefined. Since exact solutions can be obtained for the rectangle, the accuracies of these techniques can be assessed.

In this study boundary points were not placed at the corners but were

displaced a distance of one-half the integration stepsize. The method for handling the normal derivatives at the corners was based on a technique developed previously by Banaugh and Goldsmith for a two-dimensional scattering problem. The results are summarized in Table II for forty-two points taken on the boundary.

As with the circle, the agreement between the exact and numerical values is good for a rigid boundary but deteriorates when a nonzero admittance is introduced. From Table II the agreement is to four significant figures in the real part of the eigenfrequency and to within .01 in the imaginary part for a rigid wall. If the corner points are ignored the agreement is only to within about two per cent. The Gaussian integration techniques developed in the study of the circle will be applied to the rectangle to improve the accuracy of the computed eigenfrequencies for a nonzero admittance condition.

The boundary values of the acoustic potential are shown in Figure 7 along lines of constant  $x$  and  $y$ . The effect of an admittance condition on the values along the  $x$  axis is also shown. The agreement between the exact and numerical results is within one per cent.

### C. Star

In studying the star-shaped boundary, the applicability of the integral relations to a complicated geometry for which separation of variables does not apply can be assessed. The first nine eigenfrequencies and natural modes for the star are presented in Figure 8 for a rigid wall with forty-eight points taken on the surface. The most unique feature of the acoustic field for the star is the appearance of nodal points at some of the resonant modes. In the circle and rectangle nodal lines only were present and



followed one of the separable coordinates of the boundary. With the star both nodal lines and points can occur. Isometric views of the pressure fields for the third and fifth modes are shown in Figures 9 and 10.

Another unique feature of the modes of the star is the phase between the pressure oscillations at two interior points. For the modes containing nodal lines, the pressure oscillations are either in phase or 180 degrees out of phase at every point. This result was also obtained for the circle and rectangle. However, for the modes containing nodal points the phase varies continuously along lines parallel to the boundary.

Before applying a nonzero admittance condition at the boundary of the star, the computer program will be modified to use the Gaussian integration routine. The effect of the admittance will then be determined for the first five modes.

#### IV. FUTURE WORK

To complete the requirements of this research grant, the following tasks will be performed.

- (1) The Gaussian integration routine will be applied to the rectangle to determine its applicability to shapes with corners. If applicable it will then be incorporated into the program for computing the eigenfrequencies and the corresponding modes of the star for nonzero boundary admittance values.
- (2) The results for the star-shaped boundary will be checked experimentally.

- (3) The acoustic characteristics of a duct with a right-angle bend will be investigated and compared with results obtained using finite differences.
- (4) Upon completion of these tasks sometime in July, 1975, the final report will be prepared and submitted by October, 1975.
- (5) Two papers are in preparation for publication in the Journal of the Acoustical Society of America and/or the Journal of Sound and Vibration. The first will deal with the analytical techniques developed in the course of this research and the second will deal with the general effect of boundary shapes and wall conditions on acoustic properties in enclosures. Other papers may be written applying this technique to particular configurations of interest in specific problems.

The results obtained for the two-dimensional problem demonstrate that this technique is an accurate and rapid means for determining the acoustic properties of two-dimensional ducts with complicated shapes. The numerical techniques are directly applicable to both radiation and scattering problems. Because of the promise shown by this technique in two-dimensional problems, its application to three-dimensional studies is currently undergoing feasibility studies at no cost to this contract. Depending on the outcome of these studies, a logical extension of the present grant would be towards developing techniques for solving the three-dimensional problem which would extend the range of applicability to a greater number of problems in noise abatement and control.

TABLE I. EIGENFREQUENCIES FOR THE CIRCLE OF UNIT RADIUS

ADMITTANCE $y = 0 + 0i$			$y = 0.3i$		$y = 0.3$	
MODE	Numerical	Exact	Numerical	Exact	Numerical	Exact
1	1.84122 - .00010i	1.84118	1.4441 - .007029	1.4384	1.8195 + .4032i	1.8322 + .4432i
2	3.05423 - .00031i	3.05424	2.5369 - .01466i	2.5247	3.0477 + .5322i	3.0786 + .5442i
3	3.83175 - .00034i	3.83171	NOT COMPUTED	3.5510	NOT COMPUTED	3.8188 + .3095i
4	4.20135 - .00066i	4.20119	3.5816 - .02287i	3.5617	4.2057 + .6169i	4.2532 + .6315i
5	5.31783 - .00121i	5.31755	NOT COMPUTED		5.33069 + .6925i	5.3953 + .7101i
6	5.33152 - .00067i	5.33144	5.0470 - .02096i	5.0374	5.2873 + .3096i	5.3222 + .3212i
7	6.41608 - .00197i	6.41562				
8	6.70624 - .00115i	6.70613				
9	7.01567 - .00118i	7.01559				
					Numerical Using Gaussian Integration	
1					1.8324 + .4423i	1.8322 + .4432i
2					3.0791 + .5397i	3.0786 + .5442i
3					NOT COMPUTED	3.8188 + .3095i
4					4.2538 + .6199i	4.2532 + .6315i

TABLE II. EIGENFREQUENCIES FOR THE TECTANGLE WITH A RATIO OF HEIGHT  
TO WIDTH OF 0.5 AND A WIDTH OF UNITY

ADMITTANCE $y = 0$			$y = 0.3i$		$y = 0.3$	
MODE	Numerical	Exact	Numerical	Exact	Numerical	Exact
1	$3.14123 + .00004i$	3.14159	$2.5743 - .0099i$	2.5586	$3.1195 + .5974i$	$3.1416 + .5829$
2	$6.28240 - .00075i$	6.28319	$5.9176 - .0111i$	NOT COMPUTED	$6.2448 + .5906i$	$6.2832 + .5829$
3	$7.02315 - .00068i$	7.02482	$6.3816 - .0197i$	NOT COMPUTED	$7.0822 + .5707i$	NOT COMPUTED
4	$8.88326 + .00047i$	8.88576	$8.3354 - .0204i$	NOT COMPUTED	$8.8578 + .5873i$	NOT COMPUTED
5	$9.42391 - .00115i$	9.42478	$8.8697 - .0285i$	8.8419	$9.3737 + .5840i$	$9.4248 + .5829$

TABLE III. EIGENFREQUENCIES FOR THE STAR,  $y = 0$

MODE	NUMERICAL
1	$1.9492 - .0011i$
2	$2.5281 - .0007i$
3	$4.0231 - .0022i$
4	$4.5883 - .0042i$
5	$4.7319 - .0015i$
6	$5.5838 - .0007i$
7	$5.8232 - .0045i$
8	$6.7018 - .0031i$
9	$6.9968 - .0020i$



(A) Differential Helmholtz Equation

$$\nabla^2 \phi + k^2 \phi = 0$$

(B) Integral Helmholtz Equation for Interior Potential

$$\phi(P) = \frac{i}{4} \int_{\Gamma} \left\{ G(P, Q) \frac{\partial \phi(Q)}{\partial n_Q} - \phi(Q) \frac{\partial G(P, Q)}{\partial n_Q} \right\} dS_Q$$

$Q \neq P$

(C) Integral Helmholtz Equation for Surface Potential

$$\phi(T) = \frac{i}{2} \int_{\Gamma} \left\{ G(T, Q) \frac{\partial \phi(Q)}{\partial n_Q} - \phi(Q) \frac{\partial G(T, Q)}{\partial n_Q} \right\} dS_Q$$

$Q \neq T$

Governing Equation for the Green's Function

$$\nabla^2 G + k^2 G = \delta(P - Q)$$

where  $\delta$  is the Dirac delta function. The Green's function is

$$G(P, Q) = H_0^{(1)}(kr) \quad \text{for two dimensions}$$

Figure 1. Forms of the Helmholtz Equation

Discretized form of the Interior Integral Helmholtz Equation

$$\phi_m + \frac{i}{4} \sum_{i=1}^N \phi_i \left[ \frac{\partial H_0^{(0)}(kr_{im})}{\partial n_Q} + iky H_0^{(0)}(kr_{im}) \right] \Delta S_i = 0$$

Admittance Condition at the Boundary

$$\frac{\partial \phi}{\partial n} + iky \phi = 0$$

Figure 2. Discretization of the Integral Equation

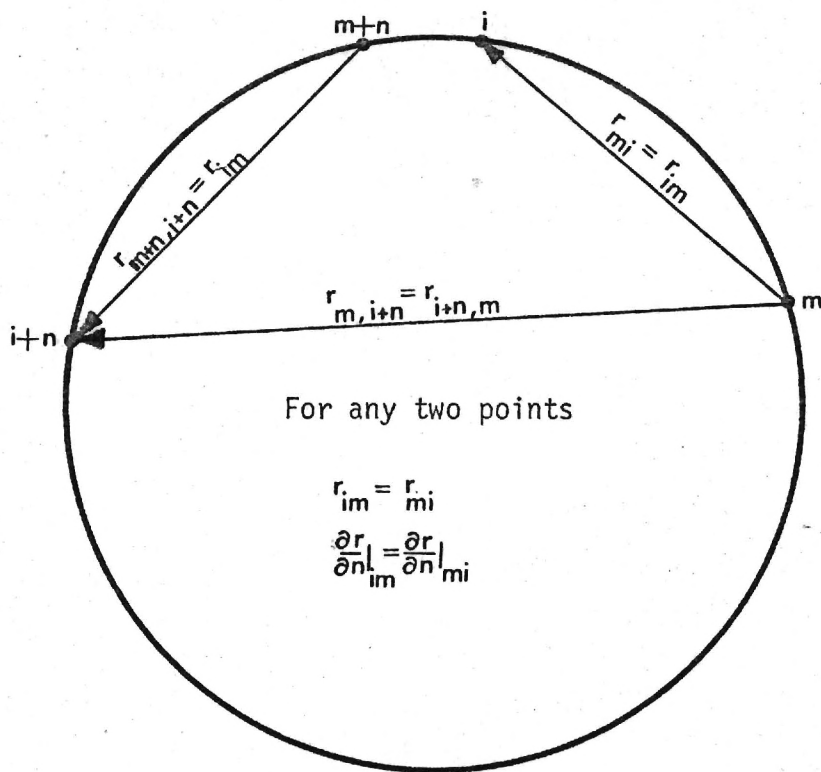


Figure 3. Use of Symmetry to Minimize Storage and Computation Requirements for a Circle.

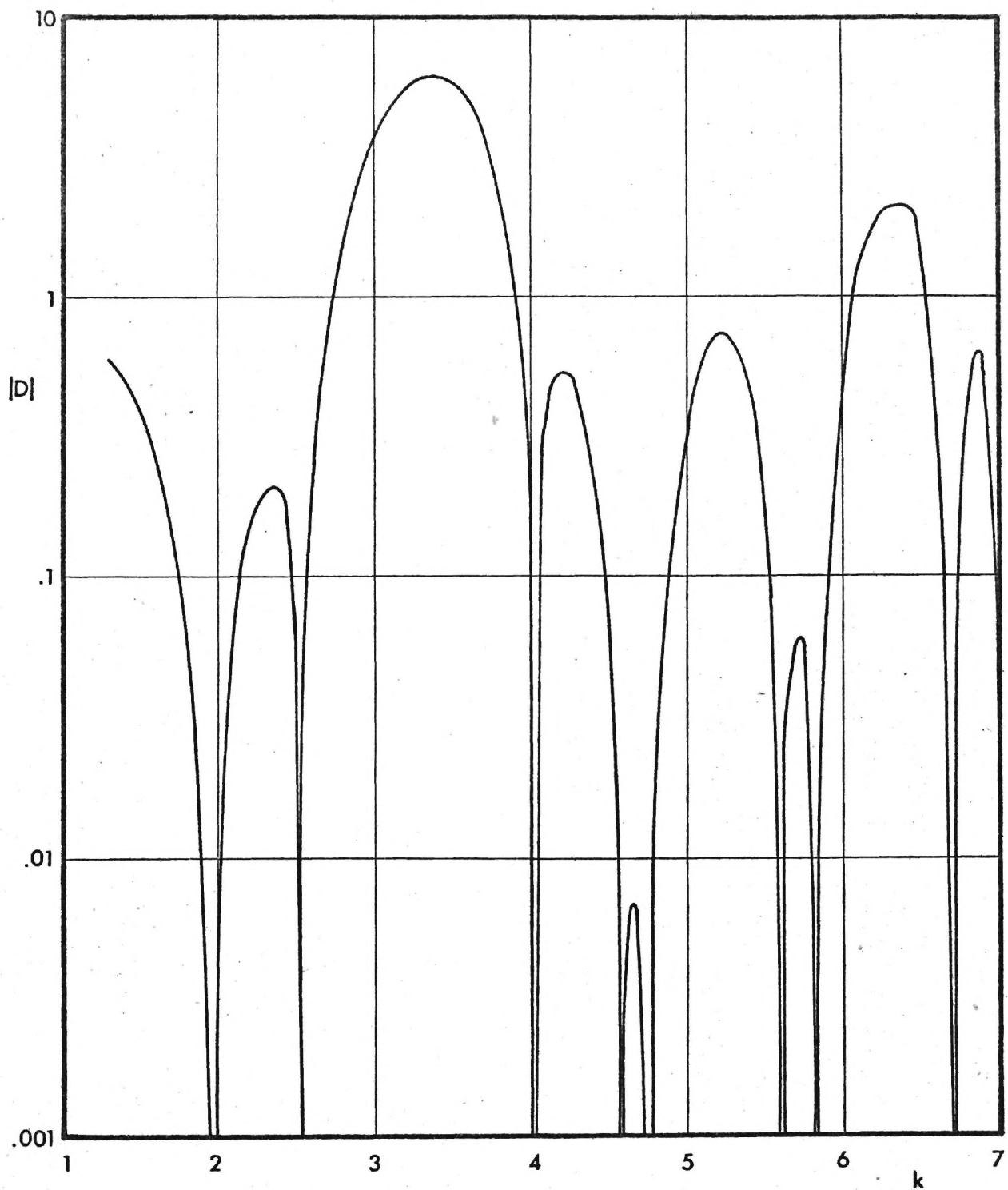


Figure 4. Plot of the Magnitude of the Determinant of the Coefficient Matrix versus Nondimensional Frequency for the Star with 48 Boundary Points.



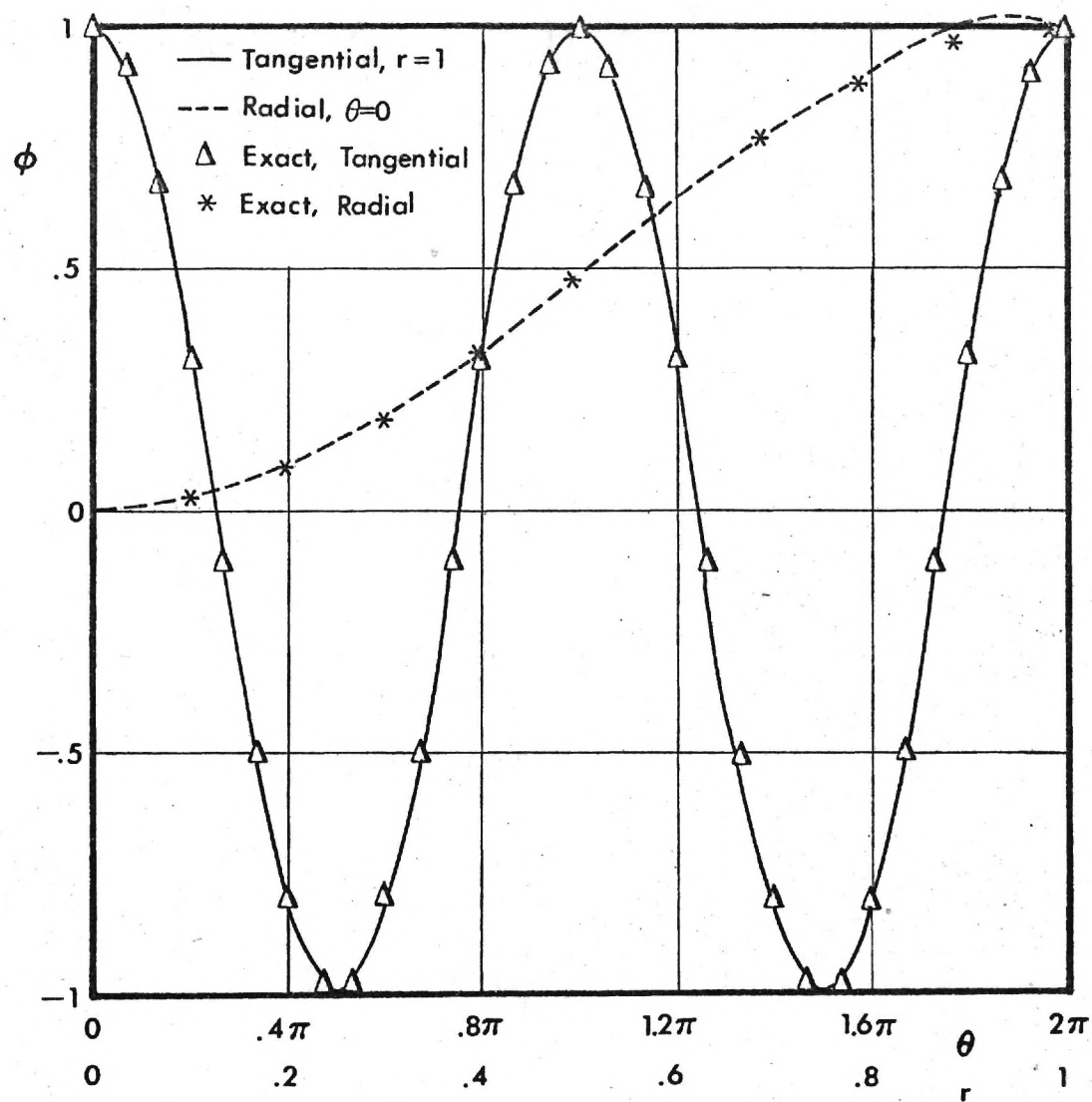


Figure 5. Second Mode for a Circle, Radial and Tangential Potential Values.  $y = 0 + 0i$

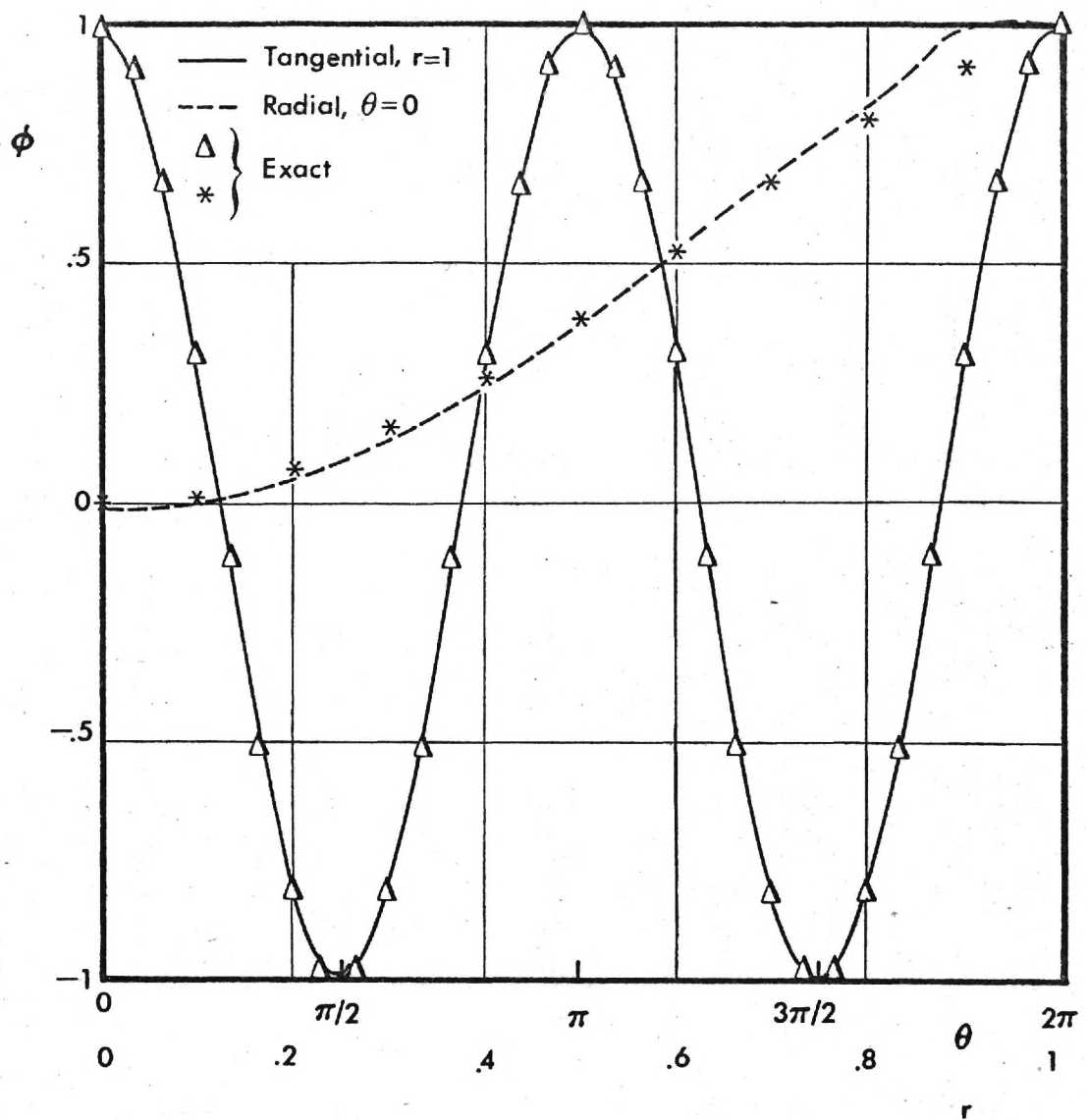


Figure 6. Comparison of Exact and Computed Potentials of a Circle for the Second Mode.  $y = .3i$

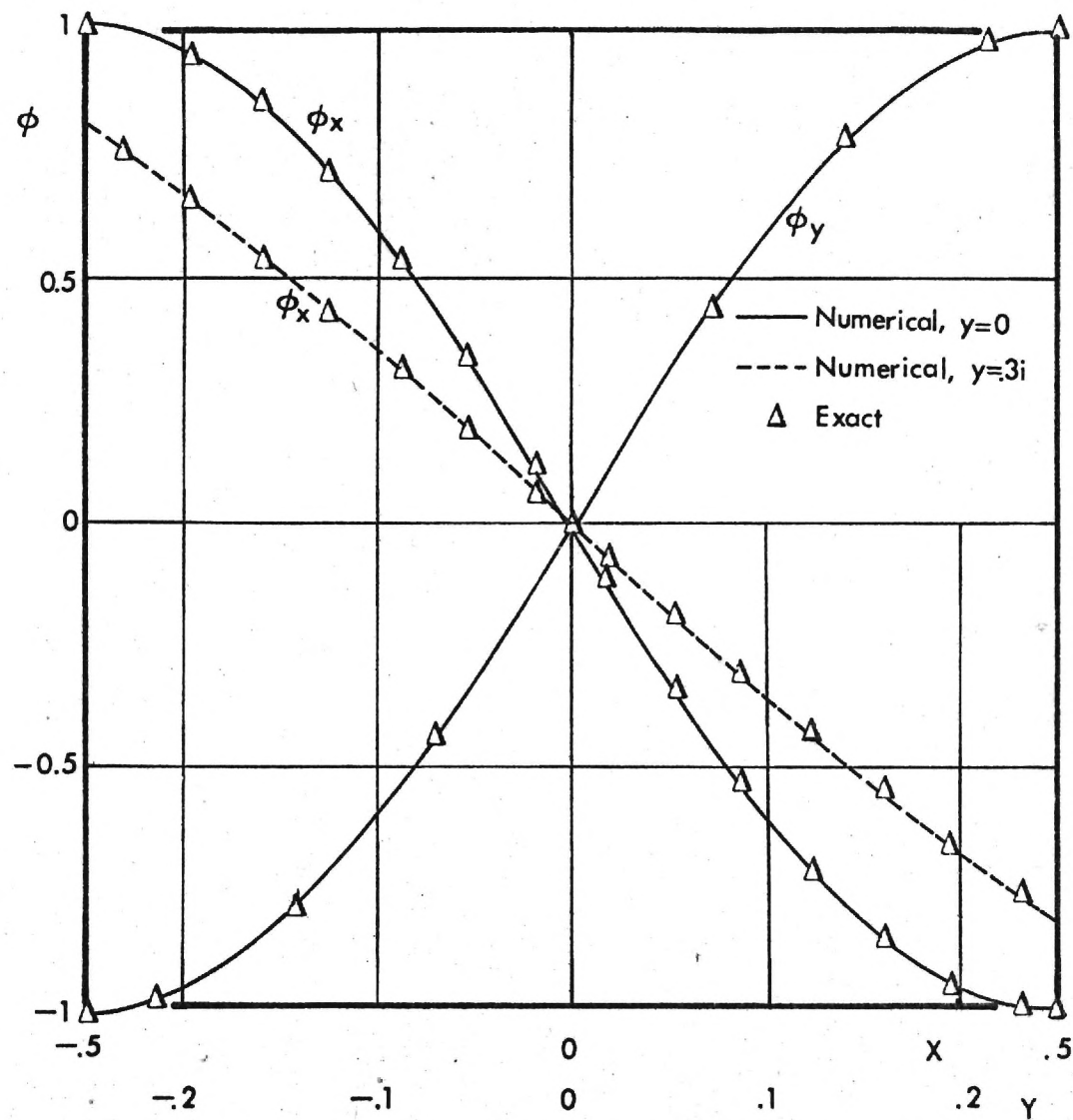


Figure 7. Comparison of the Numerical and Exact Surface Potential Values of a Rectangle for Two Admittance Conditions.

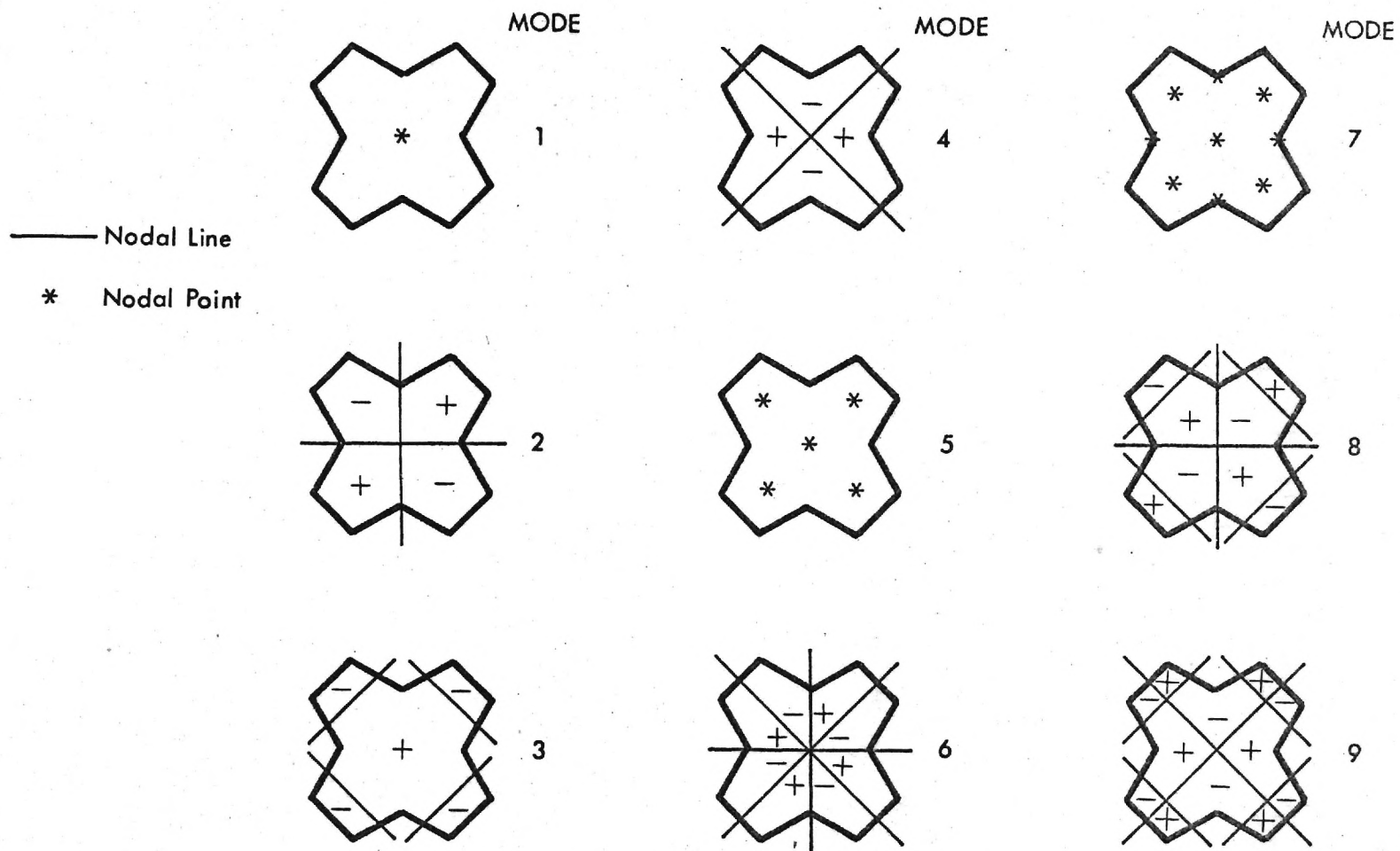


Figure 8. Nodal Points and Lines for the First Nine Modes of the Star.

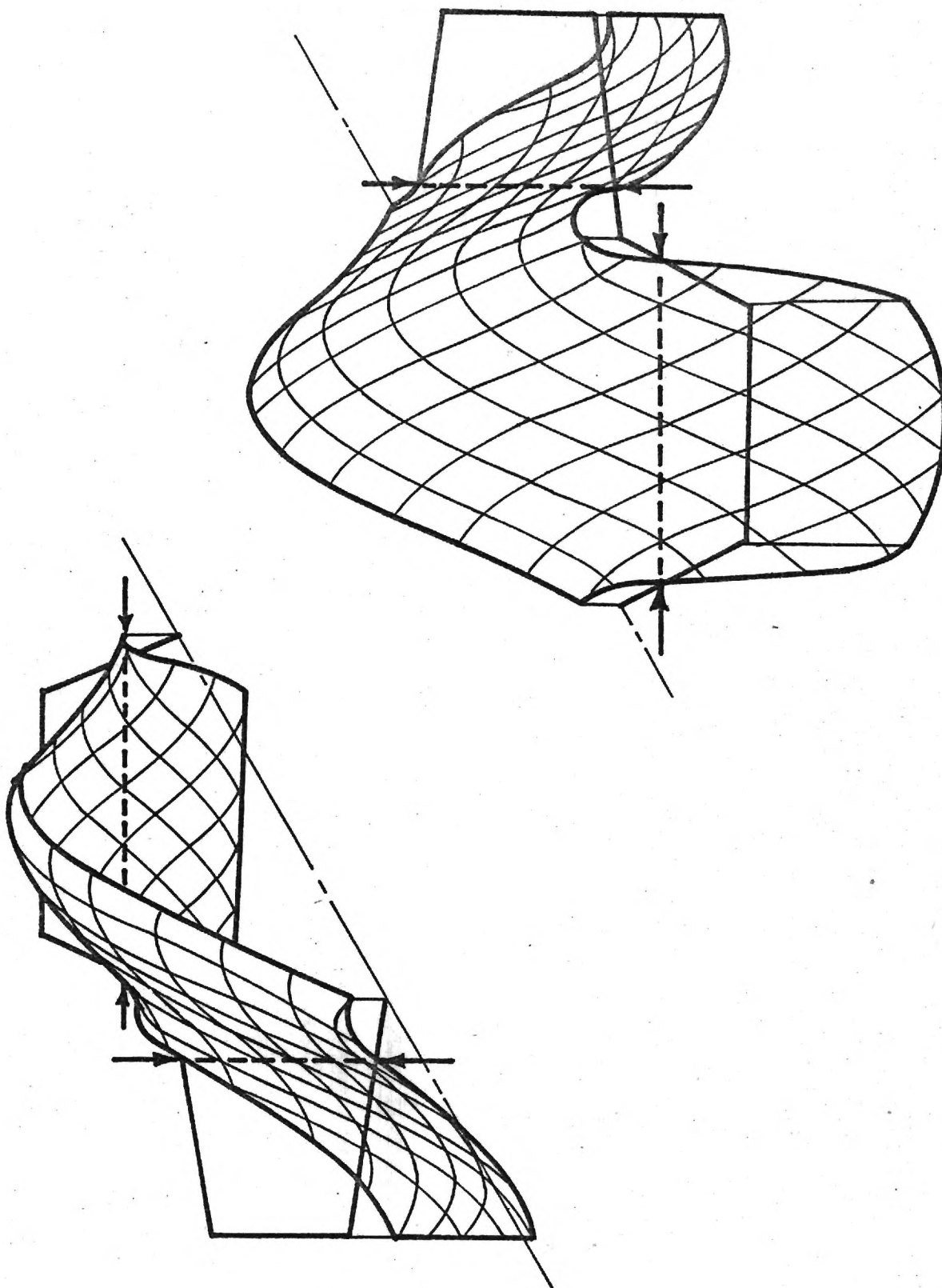


Figure 9. Altitude Chart of the Pressure Distribution for the Third Mode of the Star. Arrows Point to the Nodal Lines.



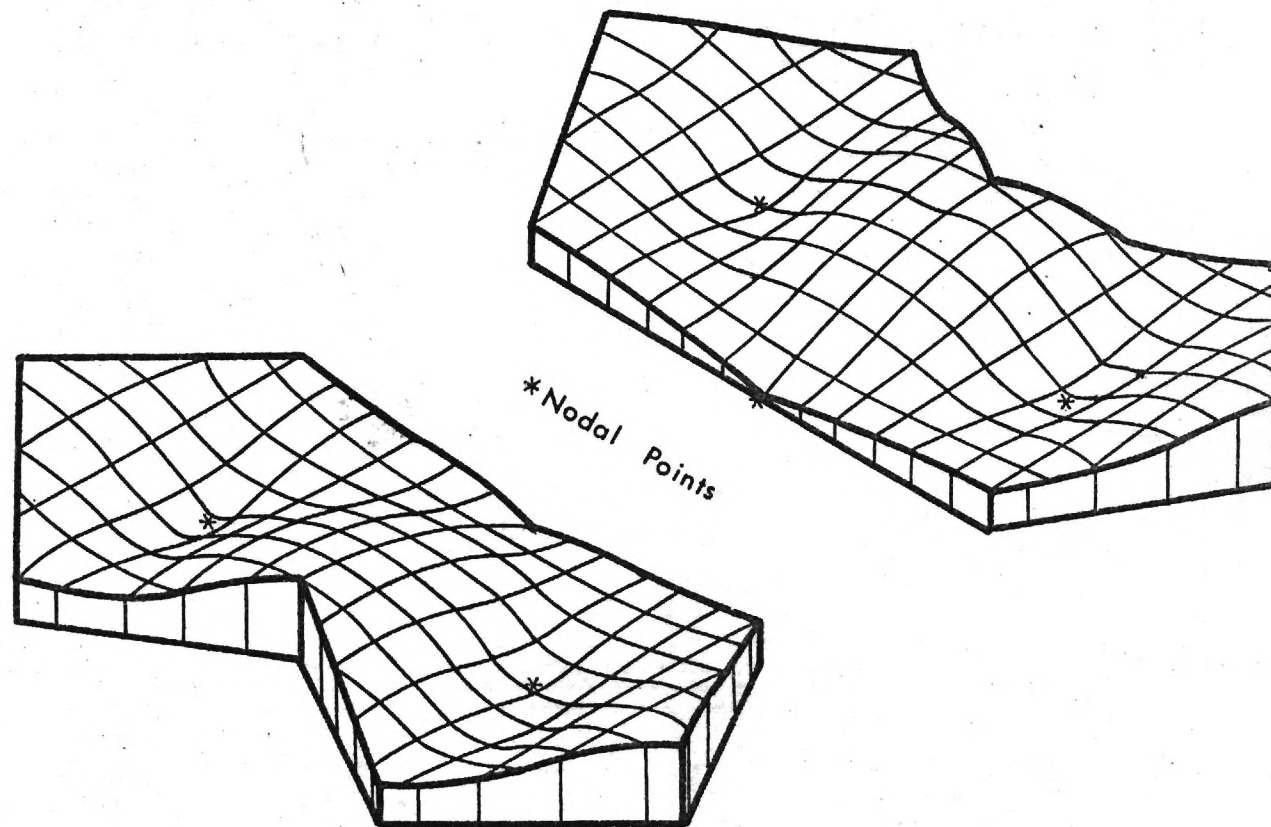


Figure 10. Altitude Chart of the Pressure Distribution for the Fifth Mode of the Star.

NATIONAL SCIENCE FOUNDATION GRANT GK-42159  
GEORGIA TECH CONTRACT NUMBER E-16-647

Research Initiation

RESONANT FREQUENCIES AND NATURAL MODES  
OF ARBITRARILY SHAPED DUCTS

FINAL REPORT FOR THE PERIOD APRIL 1, 1974 TO SEPTEMBER 30, 1975

PREPARED BY:

WILLIAM A. BELL  
PRINCIPAL INVESTIGATOR

School of Aerospace Engineering  
Georgia Institute of Technology  
Atlanta, Georgia 30332

## TABLE OF CONTENTS

SUMMARY	i
I. INTRODUCTION	1
A. Objectives	1
B. Practical Applications	1
C. Background	3
D. Research Accomplished	6
II. GOVERNING EQUATIONS	10
A. Integral Formulation	11
B. Boundary Conditions and Their Effects on the Eigenvalues	15
C. Summary	19
III. SOLUTION TECHNIQUE	20
A. Discretization of the Integral Equations	20
B. Surface Geometry and Boundary Conditions	21
C. Computation of the Coefficients of the Discretized Integral Equation	25
D. Determination of the Resonant Frequencies and Natural Mode Shapes	28
E. Summary	32
IV. RESULTS	
A. Circle	33
B. Rectangle	35
C. Star	41
D. Duct with a Right Angle Bend	51
E. Other Studies	51
F. Summary of Results	55
V. CONCLUSIONS RECOMMENDATIONS AND POSSIBLE FUTURE STUDIES	56

APPENDIX A.

Brief Description of Computer Programs

60

REFERENCES

64

## SUMMARY

The objective of the proposed research is to develop an analytical technique for the determination of the resonant frequencies and acoustic mode shapes of two-and three-dimensional cavities of arbitrary geometry with mixed boundary conditions.

To accomplish this objective, an integral formulation of the Helmholtz equation, which governs the sinusoidal wave motion of a perfect gas, is used to avoid the limitations of the finite difference and series expansion formulations currently in wide use. Using the appropriate Green's functions for the two-and three-dimensional cases the integral equations are written as finite sums which results in a system of linear algebraic equations to be solved for the acoustic potential. With the time and funding available, only two-dimensional problems are studied although application of the theory to three-dimensional problems is discussed. This system of equations is then solved using Gaussian elimination, and the eigenfrequencies and corresponding mode shapes are obtained. Since the integral formulation results in a diagonally dominant coefficient matrix, pivotal condensation is not required which results in a 25 to 50 per cent reduction in computer time.

The theory is first applied to a circle and a rectangle, for which exact solutions exist. For the circle the numerical solutions are in agreement with exact results to five significant figures for a rigid surface with thirty points taken on the boundary. For a nonrigid boundary agreement is to within two to three significant figures. The decrease in accuracy for the nonrigid boundary is caused by the appearance of a logarithmic singularity in the integral formulation and has not been studied prior to this investigation. Techniques employing Gaussian quadrature have been developed to minimize the



error associated with the logarithmic singularity. For the rectangle, techniques are developed for handling corner points where a  $1/r$ -type singularity is encountered in the integral formulation. These techniques are an improvement over ones developed previously in other studies and result in an agreement to three significant figures between numerical and exact results.

Using the numerical methods developed in the investigations with the simple geometries, results are given for a star - shaped boundary and duct with a right angle bend. For the star the appearance of nodal points instead of nodal lines in the shapes of some of the natural modes is predicted which is in agreement with experimental observations. For a duct with right-angle bend, the effect of mixed boundary conditions and a sound source is investigated. The results for the wave shapes obtained in this investigation compare favorably to the wave pattern computed using finite differences.

## I. INTRODUCTION

### A. Objectives

The objective of the proposed research is the development of a general analytical technique for the prediction of the resonant frequencies and natural modes of acoustic waves inside arbitrarily shaped ducts with mixed boundary conditions. Such a technique is needed to improve the acoustic properties of systems used in domestic applications and industry. To achieve this objective, an integral formulation of the wave equation is used because of computational advantages. The resulting expressions are solved numerically. To evaluate the accuracy of the theoretical model, it is applied to ducts with simple geometries and boundary conditions and the numerical results are compared with available exact solutions. For more complicated shapes and boundary conditions, the predicted results are compared with experimental data or published numerical values obtained by other analytical techniques.

### B. Practical Applications

The analytical model developed in this investigation is applicable to the following engineering and architectural problems for which no exact solution exists.

- (1) Room Acoustics. To establish desirable acoustic properties in rooms and auditoriums, nonuniform surface admittances (for example carpeting and draperies) and irregular shapes are employed. The theoretical model developed under this grant can be applied to this problem for determination of the acoustic characteristics of the room. Such undesirable properties as nodal points, echoes, and focal regions can

then be predicted and avoided. Also, parametric studies can be carried out to determine the most efficient use of sound absorbing material, which will reduce the cost of acoustic treatment.

- (2) Combustion Instability. This phenomenon is characterized by high amplitude waves driven by the combustion process and generally occurs at one or more of the resonant frequencies of the combustor. This problem occurs in numerous applications which involve combustion processes, such as blast furnaces, industrial heaters, afterburners, and liquid and solid propellant rocket motors. The research conducted under this grant provides a means of determining the resonant frequencies of the combustor at which instability is likely to occur. Acoustic liners designed for maximum damping at these frequencies can then be employed to minimize the possibility of unstable combustion. The shape of the combustor can also be changed. For instance, in solid propellant rocket motors, the shape of the propellant grain can be modified to stabilize the combustion process.
- (3) Electromagnetic Waves. Since the Helmholtz equation describes the spatial variation of electromagnetic waves, the techniques developed in this research are applicable to the problem of electromagnetic wave propagation in wave guides. The theory can be used to determine the resonance characteristics of these waves in irregular wave guides with mixed boundary conditions.

The numerical techniques developed can also be used to solve related integral equations which occur in the fields of heat conduction, aerodynamics and aeroelasticity.

### C. Background

A brief description of the existing analytical approaches for predicting the natural frequencies and modes of arbitrarily shaped ducts will now be presented. These studies are concerned with obtaining solutions to the Helmholtz equation which is derived from the wave equation when a sinusoidal time dependence is assumed and which describes the spatial dependence of the oscillations. This equation is included in most standard texts on differential equations of mathematical physics and has been extensively studied in both differential and integral form. To determine the resonant frequencies and natural modes of wave guides, the differential formulation is currently the most widely used.

In differential form, exact solutions of the Helmholtz equation can be obtained by separation of variables<sup>1,2</sup>. This method involves series expansions of the solutions in terms of eigenfunctions of the system. The eigenvalues are determined by the boundary conditions. Although this technique has been successfully applied to several practical problems in duct wave propagation<sup>3-9</sup>, it has the following limitations. (1) The series expansions often involve special functions which are difficult to compute. (2) At high frequencies and at the boundaries the series are slowly convergent. Therefore, a large number of terms in the series must be retained to ensure accurate results, which often requires excessive computation time. (3) The most serious limitation as far as the proposed research is concerned is that this method can only be used with special coordinate systems and boundary condit-

ions for which the separation of variables can be applied. To date only eleven suitable coordinate systems are known<sup>1</sup>. Because of these limitations, the separation of variables is not used in the research conducted under this grant.

For arbitrarily shaped bodies, the differential form of the Helmholtz equation can be solved by writing the equation in terms of finite differences<sup>1</sup>. Unlike separation of variables, this technique is not limited to ducts with simple geometries. A typical application of finite differences is given by Wynne and Plumbee<sup>10</sup> who solved for the transverse eigenvalues and eigenfunctions of an annular duct with lined walls. This technique involves the simultaneous solution of the acoustic potential value at every point within the duct. Once the potential values are known, the acoustic pressure and velocity can then be determined. To obtain sufficient accuracy, fine grid sizes must be used which necessitates large computer storage requirements. This drawback was noted by Baumeister<sup>11</sup>, Baumeister and Rice<sup>12</sup>, and Alfredson<sup>13</sup> who used this technique in studies of duct wave propagation. Because of the storage requirements this technique has only been applied to two-dimensional problems. For three-dimensional problems numerical methods capable of handling large matrices must be used which require considerable computer time and computational effort<sup>14</sup>.

For wave propagation inside arbitrarily shaped surfaces, a numerical technique must usually be employed to solve the governing equations. The integral form of the Helmholtz equation is more suitable for numerical solution. This formulation relates the value of the acoustic potential function at any point inside the surface to the values of the function at the surface. Unlike the differential Helmholtz equation which involves the simultaneous determination of the acoustic field at every point in the interior domain,



the integral formulation reduces the problem to the much simpler one of determining the wave form at the surface. Essentially, the number of dimensions of the problem is reduced by one. Thus, the computer storage required for numerically solving the integral form of the Helmholtz equation is much less than the storage requirements and associated computation times necessary for solving the differential form by finite differences.

To avoid the limitations of the differential formulation, the integral approach is employed in this research. The integral approach has been successfully applied to related acoustic problems. In determining the sound radiation field from vibrating surfaces, integral techniques have been widely used<sup>15-18</sup>. For example, Chen and Schweikert<sup>15,16</sup> employed this method to determine the radiation sound patterns for three-dimensional shapes with mixed boundary conditions. To check the accuracy of the results, they computed the radiated field produced by a piston vibrating on a sphere. For this problem an exact solution exists<sup>3</sup> and compared favorably with the numerical results. The integral formulation is also used to solve the problem of scattering by arbitrary shapes<sup>19-22</sup>. Banaugh and Goldsmith, for example, used this technique to investigate the effect of surface shape<sup>19,20</sup> on scattered sound fields. By applying this method to a circular cylinder, for which exact solutions are available<sup>3,4</sup>, and comparing the exact and numerical solutions, Banaugh and Goldsmith demonstrated the accuracy of the integral solution scheme. Although this method is capable of handling mixed boundary conditions, only surfaces with rigid boundaries were considered in References 19 and 20. The effect of mixed boundary conditions was included in a study by Liu and Martenson<sup>23</sup> of the internal acoustic pattern of a lined axisymmetric duct of arbitrary shape. Comparison of the theoretical predictions with experimental data showed gen-

erally good agreement although both the theoretical development and experimental technique are open to question. Unpublished work by Zinn and Gaylord<sup>24</sup> demonstrated the applicability of the proposed integral formulation for the determination of the natural frequencies and modes for two-dimensional shapes. In this study the accuracy of the technique was determined by comparing the natural frequencies and mode shapes with available exact solutions for a two-dimensional cylinder with rigid walls. As shown in Table 1, the agreement is to within four decimal places which is two orders of magnitude greater in accuracy than previous results obtained by solving the differential Helmholtz equations using finite differences<sup>10</sup>. In another study of Tai and Shaw<sup>25</sup>, the integral method was applied to a right triangle. The resulting eigenfrequencies compared with exact solutions to within 5 per cent and the maximum deviation between the numerically computed and exact potential fields was less than one per cent.

#### D. Research Accomplished

Because of its demonstrated success in related acoustic fields and its advantages over the differential formulation, the integral form of the wave equation is used in this study. The research accomplished under this grant is given in Figure 1. The general formulation of this problem for determining the resonant frequencies and natural modes of arbitrarily shaped bodies with mixed boundary conditions is presented in Section II. The properties of the eigenvalues are discussed, and the boundary conditions of importance in acoustic problems are presented. In Section III, numerical techniques for obtaining the solutions of the integral equations are presented and discussed. The cases investigated are presented in Section IV and include the study of a right circular cylinder, a rectangle, and a star-shaped cavity typical of solid

TABLE I.

Comparison of the Exact Values of the Resonant Frequencies and Natural Modes with the Computed Values Obtained by Solving the Integral Equations Numerically (Taken from Reference 24).

Exact Eigenvalues	40 Boundary Points	Maximum Deviation between the Exact and Numerical Values of the Surface Potential
1.84118	1.84120*	.00164
3.05424	3.05427*	.00325
3.8317	3.8329**	Not Computed
4.2012	4.2023**	Not Computed

\* Hankel function was used.

\*\* The Bessel function of the second kind was used.

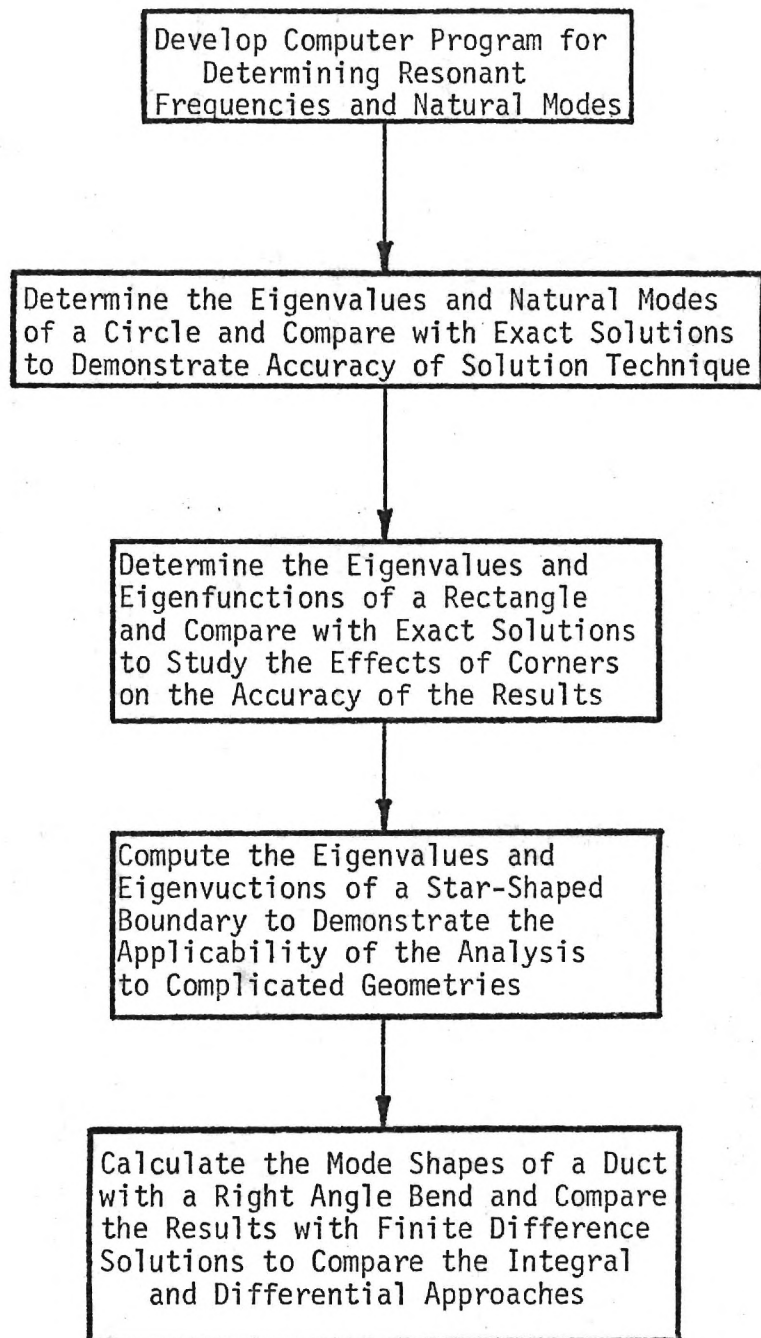


Figure 1. Research Accomplished.

propellant rocket motors. Both rigid and lined walls are considered and the results are discussed and compared with previous studies. Conclusions and recommendations are given in Section V and possible future research in this area is suggested.



## II. GOVERNING EQUATIONS

The integral formulation of the wave equation for internal wave propagation problems is developed in this section for two and three dimensions. The boundary conditions and their influence on the eigenvalues of a given surface are then discussed. For clarity, only a brief account of the derivation of the basic equations will be given in this section. For a more detailed and rigorous development, References 26 through 29 can be consulted.

Assume a frictionless, homogeneous gas, and let  $\rho_0$  and  $p_0$  be the density and pressure of the fluid at rest. Representing the acoustic pressure and particle velocity at a time  $t$  by  $p$  and  $\vec{u}$ , Euler's equation for the conservation of momentum gives

$$\rho_0 \frac{\partial \vec{u}}{\partial t} + \nabla p = 0 \quad (1)$$

The continuity equation yields the relationship

$$\frac{\partial p}{\partial t} + \rho_0 c_0^2 \nabla \cdot \vec{u} = 0 \quad (2)$$

where  $c_0$  is the speed of sound. By defining an acoustic potential function  $\psi$  such that

$$\vec{u} = \nabla \psi \quad (3)$$

Equation (1) provides the relation

$$p = -\rho_0 \frac{\partial \psi}{\partial t} \quad (4)$$

and Equation (2) results in the classical wave equation

$$\nabla^2 \psi - \frac{1}{c^2} \frac{\partial^2 \psi}{\partial t^2} = 0 \quad (5)$$

The wave equation can also be written in terms of  $p$  and  $\vec{u}$ , but it is more convenient to work with an acoustic potential function, from which both the acoustic pressure and particle velocity can readily be obtained.

Equation (5) is the wave equation for a general time dependence and can be written in integral form and solved by using retarded potentials<sup>21,28</sup>. However, for most practical problems a sinusoidal time dependence can be assumed which simplifies the problem considerably. Assume

$$\psi(\vec{r}, t) = \phi(\vec{r}) e^{-i\omega t} \quad (6)$$

Substituting Equation (6) into (5) gives the Helmholtz equation

$$\nabla^2 \phi + k^2 \phi = 0 \quad (k = \omega/c_0) \quad (7)$$

which can be solved by simpler methods not involving the use of retarded potentials.

#### A. Integral Formulation

To obtain an integral formulation of the Helmholtz equation, consider the problem shown in Figure 2. Applying Green's theorem to the Helmholtz equation<sup>1,28,29</sup> gives the following integral relation

$$\int_{\Gamma} \left[ \phi(Q) \frac{\partial G(P, Q)}{\partial n_Q} - G(P, Q) \frac{\partial \phi(Q)}{\partial n_Q} \right] dS_Q = 0 \quad (8)$$

where  $\phi$  is the acoustic potential function and  $G$  is the Green's function, which also satisfies the Helmholtz equation. The Green's function is regular inside the surface  $\Gamma$  except when  $P = Q$ . At this point  $G$  is singular. To remove this singularity from the integral given by Equation (8), point  $P$  is surrounded by a small sphere or circle  $\sigma$  of radius  $\epsilon$ . The integral will now include a term

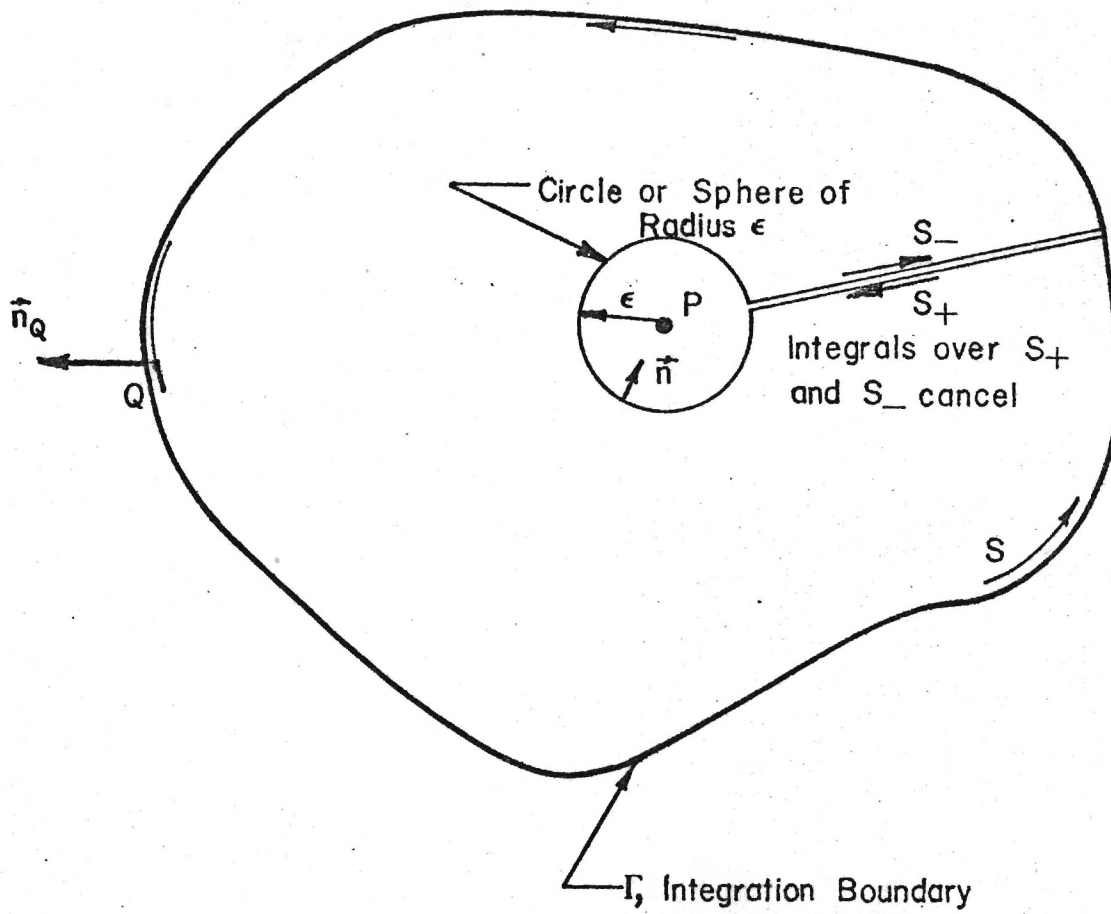


Figure 2. Integration Surface for an Interior Point

over  $\sigma$  which, on taking the limit as  $\varepsilon \rightarrow 0$ , gives

$$\phi(P) = C \int_{\substack{\Gamma \\ Q \neq P}} [G(P, Q) \frac{\partial \phi(Q)}{\partial n_Q} - \phi(Q) \frac{\partial G(P, Q)}{\partial n_Q}] dS_Q \quad (9)$$

where  $C$  is  $i/4$  for two dimensions and  $1/4\pi$  for three dimensions.

From Equation (9) the value of the acoustic potential function at any point  $P$  within the surface can be determined from the boundary values of the potential and its normal derivative. Thus, the entire wave pattern within the surface can be constructed. For arbitrarily shaped surfaces for which numerical techniques must be used to obtain a solution, Equation (9) requires much less computer storage than the differential formulation given by Equation (7). Using Equation (9) the value of the potential at each interior point can be obtained independently, whereas the method of finite differences used to solve Equation (7) requires the simultaneous solution of  $\phi$  for every interior point. To avoid the large matrices involved with finite differences, the integral formulation given by Equation (9) is used in this study.

If the values of both  $\phi$  and  $\partial\phi/\partial n$  are known at every point on the boundary, then the wave pattern can readily be determined from Equation (9). However, for most practical acoustic problems either  $\partial\phi/\partial n$  or an admittance condition relating  $\phi$  and  $\partial\phi/\partial n$  are given. Therefore, the values of acoustic potential  $\phi$  at the boundary must first be determined. The necessary relation is obtained by letting the point  $P$  approach the boundary at some point  $T$  as shown in Figure 3 to obtain the following relation<sup>26</sup>

$$\phi(T) = 2C \int_{\substack{\Gamma \\ T \neq Q}} [G(T, Q) \frac{\partial \phi(Q)}{\partial n_Q} - \phi(Q) \frac{\partial G(T, Q)}{\partial n_Q}] dS_Q \quad (10)$$

Equation (10) is applicable to a smooth boundary, but has been extended to

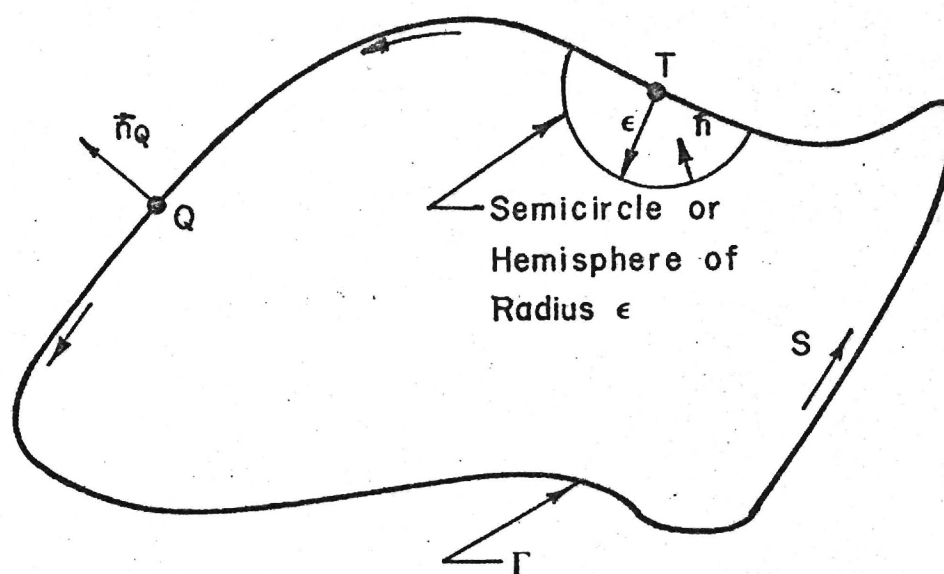


Figure 3. Surface of Integration for a Point on the Boundary

include cusps and corners<sup>19,24</sup>. To obtain the interior wave pattern, Equation (10) is first solved for the boundary values of  $\phi$ . These values are then substituted into Equation (9) to determine the acoustic potential at the interior points.

Equations (9) and (10) are applicable to both two- and three-dimensional acoustic problems. In the two-dimensional case, these equations involve line integrals; and in the three-dimensional case, the integrals are taken over a surface. Note that the dimensionality of the problem is reduced by one - a valuable simplification.

The Green's functions satisfy the following inhomogeneous forms of the Helmholtz equation with homogeneous boundary conditions<sup>1</sup>

$$\nabla^2 G + k^2 G = \delta(P - Q) \quad (11)$$

where  $\delta$  is the Dirac delta function. The Green's functions are<sup>1</sup>

$$G(P, Q) = H_0^{(1)}(kr) \quad \text{for two dimensions} \quad (12)$$

and

$$G(P, Q) = \frac{e^{-ikr}}{r} \quad \text{for three dimensions} \quad (13)$$

where  $r$  is the distance between points  $P$  and  $Q$ , and  $H_0^{(1)}(kr)$  is the zeroeth order Hankel function of the first kind.

To demonstrate the applicability of the integral solution technique, two-dimensional problems are considered in this research. In future studies it is proposed that three-dimensional and axisymmetric shapes be investigated.

#### B. Boundary Conditions and Their Effect on the Eigenvalues

The two most common boundary conditions in practical acoustic problems



are the Neumann and Robin conditions. The homogeneous Neumann condition of interest in the present eigenvalue study is

$$\frac{\partial \phi}{\partial n} = 0 \quad (14)$$

Physically, this condition means that the particle velocity is zero at the boundary which implies a perfectly reflecting, or rigid, surface. For surfaces which absorb sound, such as lined duct walls or carpeted floors, an admittance condition is usually specified, which leads to the Robin condition. Defined as the ratio of the normal component of the particle velocity to the pressure perturbation, the admittance  $y$  can be written as

$$y = \rho_0 c_0 \frac{u_n}{p} \quad (15)$$

Substituting for  $u_n$  and  $p$  from Equations (3) and (4) gives

$$y = i \frac{\partial \phi / \partial n}{k \phi}$$

or

$$\frac{\partial \phi}{\partial n} + i k y \phi = 0 \quad (16)$$

Equation (16) is the homogeneous Robin condition<sup>29</sup>. For sound absorbing materials or devices, the admittance can be either analytically determined<sup>30-32</sup> or empirically measured using the impedance tube technique<sup>33,34</sup>. The effects of a given material on the internal acoustic properties of a particular geometry can be determined by substituting the admittance of the material into Equation (16) and solving Equations (10) and (9) for the acoustic potential. Thus, the analytical technique used in this investigation is applicable to a vast number of duct and architectural acoustic problems of commercial and

domestic importance. Since the admittance of a combustion process can also be measured<sup>35</sup>, this analysis is applicable to linear combustion instability studies provided that the equations are applied to the region where the Helmholtz equation holds. By replacing the combustion process by an admittance condition, studies of combustion instability have been conducted in liquid and solid propellant combustors<sup>36,37</sup>. This research allows the extension of these analyses to more general shapes.

The general effects of the boundary conditions on the values of the resonant frequency can be determined by applying a different form of Green's theorem<sup>29</sup>. Letting  $k = k_r + ik_i$ , the following relations are obtained:

$$- \int (k_i y_r + k_r y_i) |\phi|^2 dS = (k_r^2 - k_i^2) \int |\phi|^2 dV - \int |\nabla \phi|^2 dV \quad (17)$$

$$\int (k_r y_r - k_i y_i) |\phi|^2 dS = 2k_r k_i \int |\phi|^2 dV \quad (18)$$

For two-dimensional problems, the integrals on the left-hand side of Equations (17) and (18) are line integrals and the ones on the right are surface integrals. For three dimensions the integrals are taken over the surface and volume, respectively.

From these equations, the eigenvalues must be real for a rigid surface, which satisfies the Neumann boundary condition  $\partial \phi / \partial n = 0$ . Since the admittance is zero for a rigid boundary Equation (18) indicates that either  $k_r$  or  $k_i$  must be zero. However, Equation (17) can only be satisfied for real values of  $k$ , so the eigenvalues are real. This problem has been considered by Zinn and Gaylord<sup>24</sup> for a circle and a rectangle and by Tai and Shaw<sup>25</sup> for a triangle.

For the Robin condition the following observations are made using

Equation (18).

- (1) For nonzero values of the real part of the admittance the eigenvalues are complex, and there is an exponential growth or decay in the magnitude of the wave since  $\psi(\vec{r}, t) = \phi(\vec{r}) \exp(-i\omega t) = \phi(\vec{r}) \exp[-i(k_r + ik_i) ct]$ .
- (2) For negative values of the real part of the admittance and  $y_i = 0$ , which occur for a combustion process,  $k_i$  is positive since negative values of  $k_r$  are physically meaningless. This implies that the sound amplitude increases exponentially with time.
- (3) For positive values of  $y_r$  and  $y_i = 0$  which implies a sound absorbing boundary,  $k_i$  is negative and the wave amplitude decays with time.

To determine the eigenvalues for the Robin condition, Equation (16) is substituted into Equation (10) to obtain

$$\phi(T) + 2C \int_{\substack{T \\ T \neq Q}} \phi(Q) \left[ \frac{\partial G(T, Q)}{\partial n_Q} + ik y(Q) G(T, Q) \right] dS_Q = 0 \quad (19)$$

For surfaces with spatially varying admittance conditions, the admittance is a function of  $Q$ . For most cases considered in this research,  $y$  will be assumed constant. Nontrivial solutions of this equation exist only at the resonant frequencies or eigenvalues of the surface under investigation. For the two-dimensional problem investigated under this grant the determination of the eigenvalues involves the evaluation of Hankel functions with complex arguments. The numerical techniques necessary to obtain the resonant frequencies and mode shapes are the subject of the next section.

### C. Summary

In this section integral relations are developed for computing the values of the acoustic potential function at the boundary and within the surface. The effects of the boundary conditions on the resonant frequencies are investigated, and it is shown that (1) for a rigid surface the resonant frequencies are real and (2) for nonzero values of the real part of the admittance the resonant frequencies are complex.

### III. SOLUTION TECHNIQUE

In the last section, the integral equations were developed which describe the interior acoustic field of a surface with arbitrary shape and mixed homogeneous boundary conditions. Nontrivial solutions exist only at the resonant frequencies of the system. The numerical solution technique for solving the two-dimensional equations to obtain the resonant frequencies and natural mode patterns is presented in this section and can be divided into four parts. The first is the discretization of the integral equation into a corresponding system of linear, algebraic equations in  $\phi$  suitable for solution on a computer. The second part is the specification of the geometry and boundary conditions. The third is the computation of the coefficients of the system of equations. The final part is the determination of the eigenfrequencies and eigenmodes of the geometry under consideration.

#### A. Discretization of the Integral Equations

In two dimensions, Equation (19) involves a one-dimensional integral about the boundary line. For this type of problem several numerical integration techniques<sup>38,39</sup> are available for discretizing this equation. The simplest is the trapezoidal rule which has been shown to yield excellent results in previous studies with this type of integral<sup>19,24,25</sup>. Using this numerical integration scheme, Equation (19) becomes

$$\phi_m + \frac{i}{2} \sum_{\substack{j=1 \\ j \neq m}}^N \phi_j \left[ \frac{\partial H_0^{(1)}(kr_{jm})}{\partial n_j} + ik y_j H_0^{(1)}(kr_{jm}) \right] \Delta s_j = 0 \quad (20)$$

where one equation for  $\phi$  is obtained for each value of  $m$  and  $m$  is varied from 1 to  $N$ . Equation (2) was initially used in this investigation to generate  $N$

equations for  $\phi$  and accurate results were obtained when the admittance  $y$  was zero everywhere on the boundary<sup>40</sup>. In previous studies of this problem<sup>19,24,25</sup> the admittance was taken to be zero. However, when a nonzero admittance is assumed, this technique gives inaccurate results because of a logarithmic singularity in  $H_0^{(1)}(kr_m)$  when the point  $j$  approaches  $m$ . This singularity is discussed further in Section III (C). To overcome the inaccuracies involved, a modification of Equation (20) is used and is given by Equation (21).

$$\phi_m \left\{ 1 + i/2 \int_{S_{m-1/2}}^{S_{m+1/2}} \left[ \frac{\partial H_0^{(1)}(kr_{o1/2})}{\partial n_{1/2}} + ik y_m H_0^{(1)}(kr_{o1/2}) \right] dS \right\} \\ \frac{i}{2} \sum_{\substack{j=1 \\ j \neq m}}^N \phi_j \int_{S_{j-1/2}}^{S_{j+1/2}} \left[ \frac{\partial H_0^{(1)}(kr_{jm})}{\partial n_j} + ik y H_0^{(1)}(kr_{jm}) \right] dS = 0 \quad (21)$$

In both Equations (20) and (21) the values of  $\phi$  are assumed to be constant over each of the  $N$  subintervals. The difference is the method by which the terms involving the Hankel functions are evaluated. In Equation (20) an average value is computed over each of the subintervals based on  $r_{jm}$ . With Equation (21) these terms are integrated numerically from  $r_{j-1/2,m}$  to  $r_{j+1/2,m}$  using Gaussian quadrature<sup>39,40</sup> to obtain more accurate values. This type of formulation has been used before using trapezoidal instead of Gaussian quadrature formulas<sup>18</sup>. In the present study a reduction in error of two orders of magnitude in the numerical results was achieved using Equation (21) instead of Equation (20) for a nonzero admittance<sup>40</sup>.

#### B. Surface Geometry and Boundary Conditions

The first step in solving Equation (21) is the determination of the coefficients if  $\phi_j$  and  $\phi_m$ . These coefficients depend upon the surface geome-



try through the terms  $\partial/\partial n_j$ ,  $r_{jm}$ , and  $\Delta S_j$ . By specifying the admittance  $y$  over every subinterval  $j$ , the effect of the boundary conditions are included in the evaluation of the coefficients.

To solve for the terms involving the surface geometry, the first expression inside the integrals of Equation (21) is written as

$$\begin{aligned}\frac{\partial H_0^{(1)}(kr)}{\partial n} &= \frac{\partial H_0^{(1)}(kr)}{\partial r} \frac{\partial r}{\partial n} \\ &= -kH_1^{(1)}(kr) \frac{\partial r}{\partial n}\end{aligned}$$

Thus, Equation (21) becomes

$$\begin{aligned}\phi_m \left\{ 1 - ik/2 \int_{S_{m-1/2}}^{S_{m+1/2}} [H_1^{(1)}(kr_{o1/2}) \frac{\partial r}{\partial n_m} - iy_m H_0^{(1)}(kr_{o1/2})] ds \right\} \\ - \frac{ik}{2} \sum_{\substack{j=1 \\ j \neq m}}^N \phi_j \int_{S_{j-1/2}}^{S_{j+1/2}} [H_1^{(1)}(kr_{jm}) \frac{\partial r}{\partial n_j} - iy_j H_0^{(1)}(kr_{jm})] ds = 0\end{aligned}\quad (22)$$

The expressions for  $\partial r/\partial n_j$ ,  $r_{jm}$ , and  $ds$  can be written in parametric form. This type of representation has been used in previous studies using simple geometries<sup>17-20,24,41,42</sup>. By taking advantage of symmetry, considerable savings in computer storage and computation times were achieved. In fact, Greenspan and Werner<sup>42</sup> showed that for a circle Equation (22) can be reduced to a single equation instead of a system of equations which could readily be solved to obtain the acoustic field. In the study by Tai and Shaw<sup>25</sup>, the method of images<sup>1</sup> was used to greatly reduce the number of points necessary to compute eigenfrequencies and eigenmodes of a family of triangles. Although these studies point out valuable simplifications which can be made in applying the integral formulation to a particular problem, the techniques used are not

applicable to more general problems involving complicated geometries and non-uniform boundary conditions.

In the present study, the expressions for the geometric variables are written in parametric form only for the circle. In the rest of the configurations considered, a general formulation is used. The fact that a parametric representation cannot be used in general cases is not a serious drawback - in fact, it somewhat simplifies the formulation. Consider the general problem depicted in Figure 4. By specifying the  $x$  and  $y$  coordinates at the midpoint of each of the subintervals, the distance  $r_{jm}$  is readily computed from the expression from analytical geometry

$$r_{jm} = \sqrt{(x_j - x_m)^2 + (y_j - y_m)^2} \quad (23)$$

The expression for  $\partial r / \partial n_j$  can then be obtained since it represents the dot product of the gradient of  $r$  and the normal at  $j$ . Thus,

$$\frac{\partial r}{\partial n_j} = \frac{(x_j - x_m) n_{xj} + (y_j - y_m) n_{yj}}{r_{jm}} \quad (24)$$

where  $n_{xj}$  is the component of the normal vector  $j$  in the  $x$  direction (or the cosine of the angle between the normal vector and the  $x$ -axis) and  $n_{yj}$  is the corresponding  $y$  component (the sine of the angle between the normal vector and the  $y$ -axis). The line segment length  $\Delta S_j$  is simply

$$\Delta S_j = \sqrt{(x_{j+1/2} - x_{j-1/2})^2 + (y_{j+1/2} - y_{j-1/2})^2} \quad (25)$$

or, for  $N$  equally spaced subintervals,

$$\Delta S_j = L/N \quad (26)$$

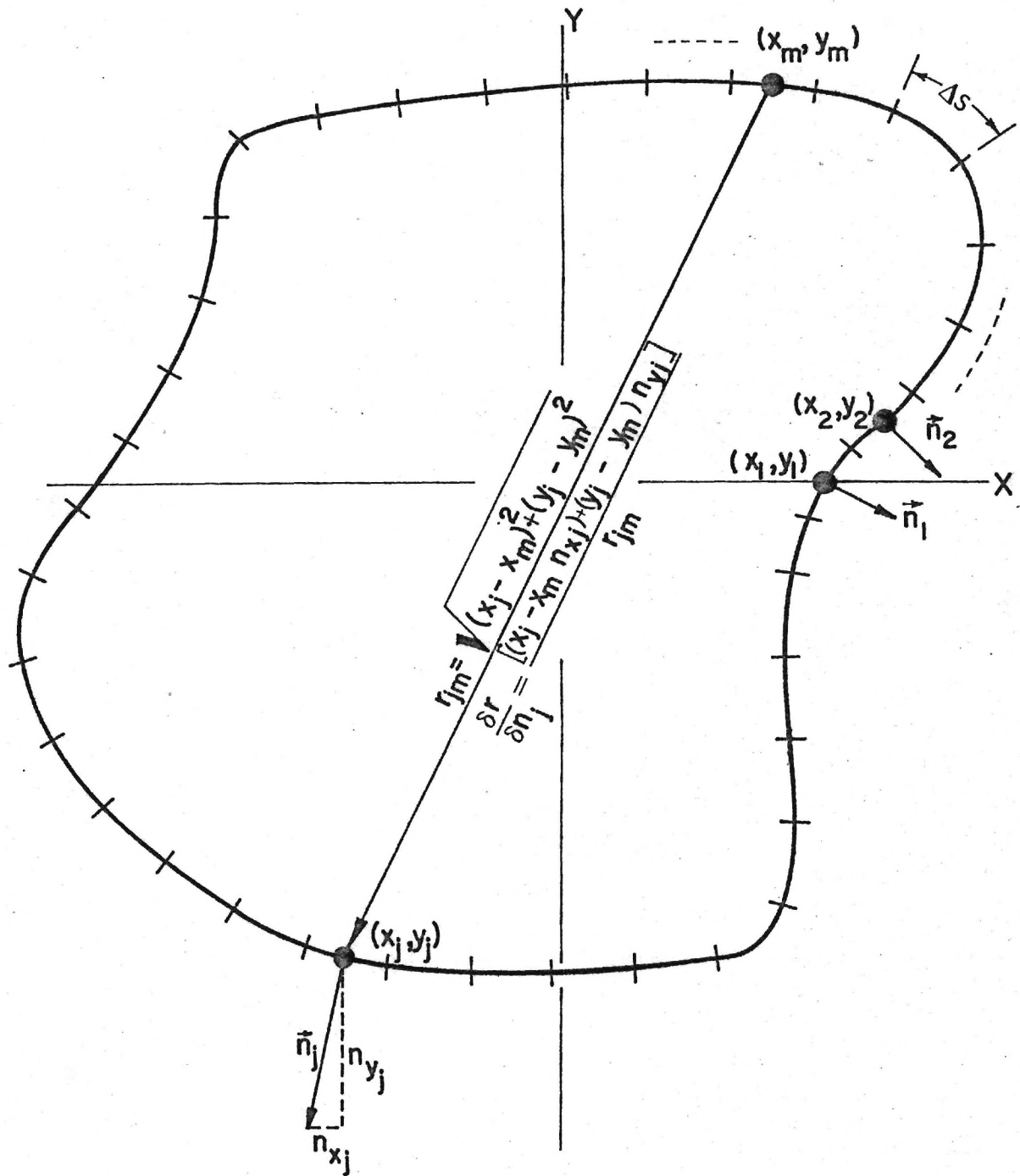


Figure 4. Geometric Considerations for General Problem.

where  $L$  is the length of the perimeter of the surface.

To determine the geometric parameters appearing in the coefficients in Equation (22), the only requirement is to specify the  $x$  and  $y$  coordinates and the normal at each of the  $N$  subintervals. Thus, it is unnecessary to use parametric equations or to store the distances  $r$  and normal derivatives  $\partial r/\partial n$  in  $N \times N$  arrays which saves considerable computer storage. However, using symmetry it is possible to reduce the size of the arrays for  $r$  and  $\partial r/\partial n$  by as much as a factor of  $N$  in the case of the circle. This saves computation time for the eigenvalue problem considered in this study. By storing  $r$  and  $\partial r/\partial n$  in arrays, these parameters must only be computed once for a particular geometry for all values of wave number  $k$  which saves computation time. The programmer can choose the method he wants to employ. If storage is a problem only  $x$ ,  $y$ ,  $\Delta S$ , and the normal vector components need be stored and the geometric parameters can be computed from Equation (23) through (26).

Another advantage of the formulation given by Equation (22) is the relative ease of taking uneven subintervals which is done in this study for the star. If finite differences are employed, considerable difficulties can be encountered<sup>38</sup>.

### C. Computation of the Coefficients of the Discretized Integral Equation

Once the geometry has been specified, the coefficient of  $\phi$  in Equation (22) can be determined by evaluating the Hankel functions  $H_0^{(1)}(kr_{jm})$  and  $H_1^{(1)}(kr_{jm})$ . There are two problems in determining these functions: the first is a rapid, accurate method for computing them over a wide range of the argument  $kr_{jm}$ ; and the second is the singularity associated with each function as  $r_{jm}$  approaches zero.

To compute the Hankel functions two routines have been used in this study. The first consists of series expansion using standard formulas for

the Hankel function with complex arguments<sup>39,43</sup>. A sufficient number of terms is taken to satisfy a specified degree of accuracy. For large values of the argument -  $|kr_{jm}|$  greater than 10 - asymptotic expansions are used<sup>39</sup>. The series tend to be slowly convergent for values of  $|kr_{jm}|$  close to 10 which leads to excessive computation times. There is no problem with the accuracy achieved, however, since the Hankel functions of orders zero and one which are of interest in this study are well behaved.

To minimize time, a different series expansion which is developed by Hitchcock<sup>44</sup> is used for determining these functions in the studies of the rectangle, star, and duct with a right-angle bend. With this formulation accuracies of  $10^{-10}$  or greater are achieved with only nine terms or less in the series expansion. Reductions of up to 50 per cent in computer times can be achieved with this formulation.

The major problem in evaluating the terms within the integrals in Equation (22) is the singularities associated with the Hankel functions as  $r_{jm}$  approaches zero; that is, as the point  $j$  approaches  $m$  in Figure 4. The first order Hankel function  $H_1^{(1)}$  has a  $1/r$  - type singularity whereas the zeroeth order function has an  $\ln r$  - type of singularity<sup>39</sup>. Methods for handling these singularities will now be presented.

The terms involving the first order Hankel function which has a  $1/r$  - type singularity can be written as

$$\lim_{r \rightarrow 0} H_1^{(1)}(kr) \frac{\partial r}{\partial n} \sim \lim_{r \rightarrow 0} \frac{1}{r} \frac{\partial r}{\partial n}$$

Banaugh and Goldsmith<sup>19,20</sup> show that for a smooth surface this limit is identically zero. Also, for a corner point where two straight lines intersect,  $\frac{\partial r}{\partial n}$  is identically zero on either side of the corner point. So, although the

first order Hankel function behaves like  $1/r$  as  $r$  approaches zero, this poses no problem in the numerical integration because of the  $ar/\partial n$  term.

The logarithmic singularity which occurs in the zeroeth order Hankel function has not been studied prior to this investigation since previous analyses have only dealt with rigid surfaces for which the admittance is identically zero. Because  $H_0^{(1)}$  is multiplied by  $y$ , as seen from Equation (22), this singularity does not arise when  $y = 0$ . However, in the present investigation which involves nonzero admittance values numerical integration techniques must be employed which can give accurate values of integrals of the form

$$\int_0^a \ln r \, dr$$

Such a technique can be found in Reference 39. It involves a Gaussian quadrature formula specifically derived for integrals of this form. Using this formula gives an error reduction of two orders of magnitude over the trapezoidal integration schemes previously used<sup>19,20,24,25,41,42</sup>. It is only necessary to use the logarithmic Gaussian formula over the interval about the point  $m$ . Around the other points the standard Gauss-Legendre quadratures provide sufficient accuracy in evaluating the integrals over each of the sub-intervals.

Using these techniques the coefficients in Equation (22) can now be determined, and the eigenfrequencies and surface potential distribution can then be obtained. Once the surface values are known, the internal values can then be found from the discretized form of Equation (9) which is

$$\phi_p = \frac{i}{4} \sum_{j=1}^N \phi_j \int_{S_{j-1/2}}^{S_{j+1/2}} [H_1^{(1)}(kr_{pj}) \frac{\partial r}{\partial n_j} + iky_j H_0^{(1)}(kr_{jp})] \, ds \quad (27)$$



where  $p$  is an internal point, the  $\phi_j$ 's are the surface potential values, and  $r_{pj}$  is the distance from the interior point to the  $j$ th surface point.

It was noted by Greenspan and Werner<sup>42</sup> that if the interior point  $p$  is close to the boundary, inaccuracies arise. In computing interior points the  $1/r$  singularity in  $H_1^{(1)}(kr)$  causes problems here because  $\partial r / \partial n$  now is of order unity. They overcame this difficulty by using finite elements to obtain points for distances within one surface subinterval length of the boundary. In the present investigation using the interior analog of Equation (21) errors of 5 per cent occur for a rectangle when an interior point is one-half of a surface subinterval length away from the boundary. However, using Equation (27) with a three-point Gauss-Legendre quadrature to evaluate the integrals over each of the subintervals, the accuracy achieved is of the same order as the computed surface potential. Thus, Equation (27) provides accurate potential values for interior points near the boundary and eliminates the need to employ finite differences there.

#### D. Determination of the Resonant Frequencies and Natural Mode Shapes

Once the coefficients of the surface potential at each discrete point on the surface have been determined, the values of the nondimensional frequency  $k$  for which the determinant of the coefficient matrix is zero can be found. These values of  $k$  correspond to the resonant frequencies or eigenvalues of the duct under consideration.

Because  $k$  appears both as a multiplicative factor and as part of the argument of the Hankel function as shown in Equation (22), the problem is a nonlinear matrix eigenvalue problem. The numerical techniques available to solve for a linear matrix eigenvalue<sup>45,46</sup> cannot guarantee convergence.

This problem is resolved in the present study by employing a quadratic

interpolation algorithm<sup>38,47</sup> which is rapidly convergent and is capable of computing complex zeroes for complicated functions which cannot be written explicitly. To find an eigenvalue three starting values must be assumed. For the case of a rigid wall, the eigenvalues are real numbers, so successive real values of  $k$  are assumed until the magnitude of the coefficient matrix determinant reaches a minimum. The determinant is computed using a complex Gauss-Jordan elimination technique and since the resulting coefficient matrix is diagonally dominant, pivotal condensation is not required which saves computation time. The minimum value of  $k$  along with the preceding and succeeding values are then used as the three starting points in the quadratic interpolation scheme. A typical plot of the magnitude of the determinant of the coefficient matrix versus  $k$  is given in Figure 5 for the star-shaped geometry. The values at which the determinant is minimized correspond to the natural frequencies.

For a general complex admittance at the boundary,  $k$  is complex which necessitates a search for the initial values of  $k$  in the complex plane. The algorithm first proposed for this investigation<sup>48</sup> did not work. The proposed method consists of taking successive values of the real part of  $k$  until a minimum value of the determinant is reached. At that point successive values of the imaginary part of  $k$  are taken until a minimum value of the determinant is found. The quadratic interpolation method is then employed to find the eigenfrequency. However, the determinant increases uniformly with increasing values of the real part of  $k$  for some of the shapes with a complex admittance at the boundary.

The algorithm successfully employed in this investigation is based on the following observations. For a pure imaginary value of the admittance,  $k_i$ ,

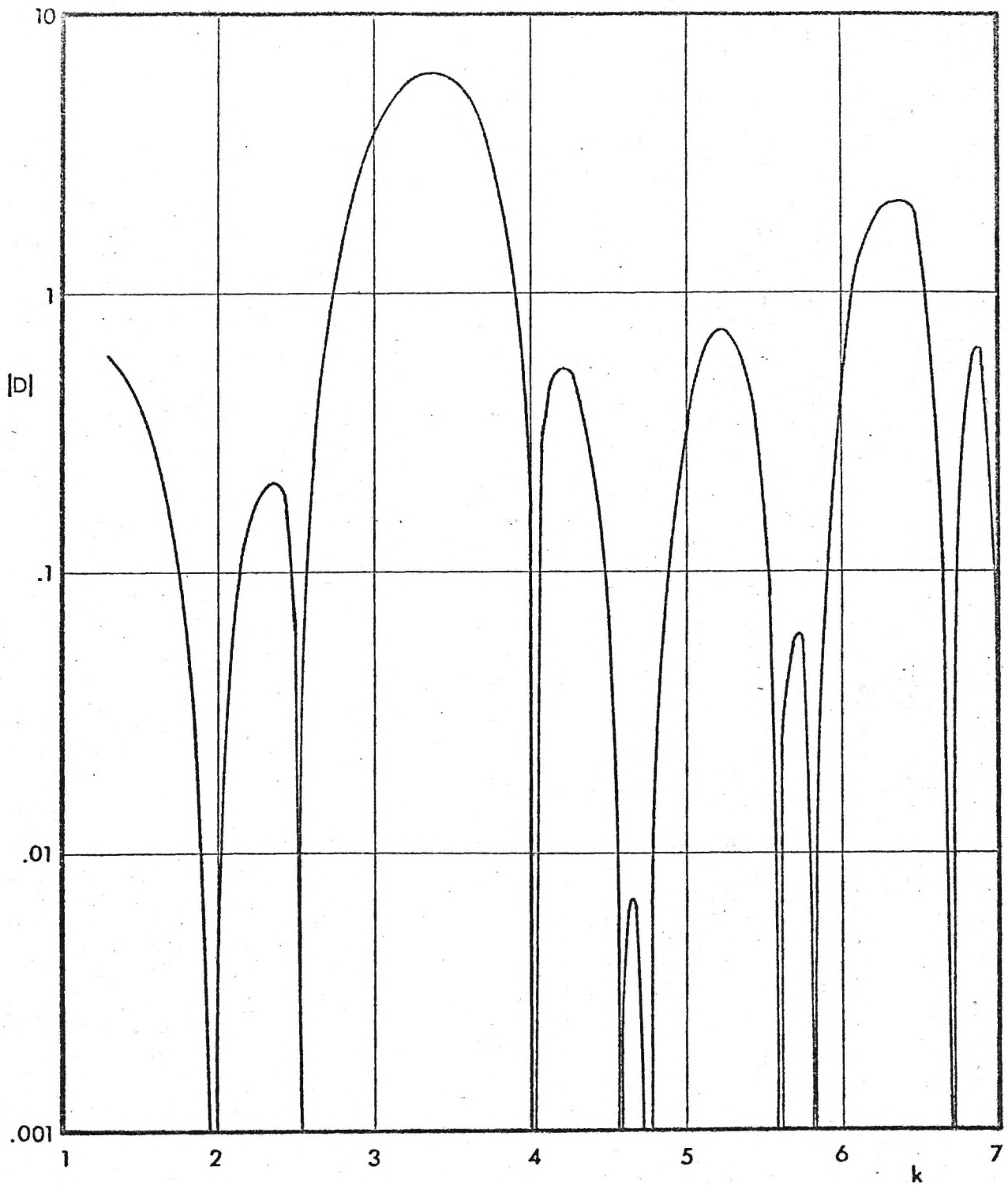


Figure 5: Plot of the Magnitude of the Determinant of the Coefficient Matrix versus Nondimensional Frequency for the Star with 48 Boundary Points.

the imaginary part of  $k$  is zero; and only  $k_r$  the real part of  $k$ , is affected. On the other hand, when the admittance is a real number, a slight shift in  $k_r$  is detected but  $k_i$  is mainly affected. Based on these observations, the following algorithm is used for a complex admittance condition.

- (1) First, take the admittance value as  $y = 0 + iy_i$ . Compute the determinant at successive values of  $k_r$  until a minimum is found. If the value of  $k$  is known for the zero admittance, it is helpful to know that negative values of  $y_i$  tend to increase the rigid wall eigenfrequency whereas positive values of  $y_i$  decrease the value.
- (2) Once  $k_r$  is found for  $y = 0 + iy_i$  at which the determinant is a minimum, let  $y = y_r + iy_i$ . Keeping  $k_r$  constant take decreasing negative values of  $k_i$  if  $y_r$  is negative or increasing positive values of  $k_i$  if  $y_r$  is positive until a minimum value of the determinant is reached.
- (3) Use the preceding and succeeding values of  $k_i$  to start the quadratic interpolation.

Using this algorithm, the eigenfrequencies for a complex admittance can be computed and is used with success for the geometries investigated under this grant. Computation times for determining an eigenfrequency and the potential distribution of the natural mode the boundary on the grantee-owned UNIVAC 1108 computer range from ten seconds for the circle to sixty seconds for the star. Since this investigation is the first attempt to determine the eigenfrequencies of complicated geometries with complex admittances using the integral approach, comparisons of computation times using other algorithms cannot be made.

To determine the resonant mode shape at a given eigenfrequency, the equations are normalized with respect to one of the surface potentials and reduced using a Gauss-Jordan matrix reduction scheme for complex coefficients. The interior points can then be found by employing Equation (27). To compute the mode shapes, from five to sixty seconds of computation time are required for nine to fifty-two interior points, respectively. In these calculations, techniques for taking advantage of symmetry have been developed to reduce time and storage requirements.

#### E. Summary

In this section the solution technique is presented and consists of (1) discretization of the integral equations given in Section II, (2) specification of the surface geometry and boundary conditions, (3) computation of the Hankel functions with their inherent singularities as the argument approaches zero, and (4) determination of the resonant frequencies and natural modes. The major achievements are (1) the development of a discretization procedure for the integral equations which gives accurate results for general boundary conditions, (2) the derivation of necessary geometric parameters which are not based on parametric formulations but can be used for general shapes, (3) improved methods for computing the integrals of the Hankel functions numerically which minimize errors associated with their singularities, and (4) development of an algorithm for computing complex eigenfrequencies.



#### IV. RESULTS

Using the numerical techniques described in the last section, solutions have been obtained for the resonant frequencies and natural modes of a circle, rectangle, and star and have resulted in two publications<sup>49,50</sup>. A third publication has been accepted<sup>51</sup>. To demonstrate the accuracy of the numerical technique, the approximate results obtained in this study for the circle and rectangle are compared with exact computation. In addition, the wave structure of a duct with a right angle bend is computed and compared with results obtained using finite differences.

The computer programs used to obtain these results are described in Appendix A. These programs are based on the formulations developed in Section II.

##### A. Circle

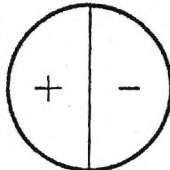
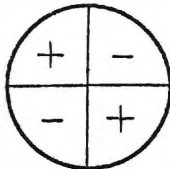
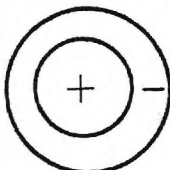
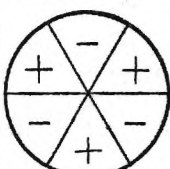
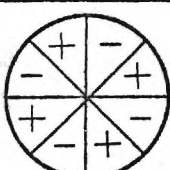
For a circle, comparisons between exact and numerical solutions are presented in Table I. In this table the numerical and exact eigenfrequencies are tabulated for three admittance values -  $y = 0$ ,  $y = .3i$ , and  $y = .3$  with thirty points taken on the boundary. A computer program for determining the exact values was developed. The best agreement between the computed and exact results occurs at the zero admittance condition. The real part of the eigenfrequencies compare to five significant figures and the imaginary parts are accurate to .001 for the first five modes. When a nonzero admittance condition is introduced, the accuracy is reduced to three significant figures in the real part and to .01 in the imaginary part of the eigenfrequencies.

As mentioned in Section II-D, the real part of the admittance has a pronounced effect on  $k_i$  while  $k_r$  is relatively unaffected. However, the



TABLE I.

Eigenfrequencies and Natural Modes of a Circle for Various Admittance Values

MODE SHAPE		ADMITTANCE VALUE		
		$y = 0 + 0i^*$	$y = 0.3 + 0i$	$y = 0 + 0.3i^*$
	COMPUTED	$1.84122 - 0.0001i$	$1.8324 + 0.4423i$	$1.4441 - 0.007i$
	EXACT	1.84118	$1.8322 + 0.4432i$	1.4384
	COMPUTED	$3.05423 - 0.0003i$	$3.0791 + 0.5397i$	$2.5369 - 0.015i$
	EXACT	3.-5424	$3.0786 + 0.5442i$	2.5247
	COMPUTED	$3.83175 - 0.0003i$	Not Computed	Not Computed
	EXACT	3.83171	$3.8188 + 0.3095i$	3.5510
	COMPUTED	$4.20135 - 0.0007i$	$4.25380 + 0.6199i$	$3.5816 - 0.023i$
	EXACT	4.20119	$4.2532 + 0.6315i$	3.5615
	COMPUTED	$5.31783 - 0.0012i$	Not Computed	Not Computed
	EXACT	5.31755	$5.3953 + 0.7101i$	4.5767

\* Numerical Results Obtained Using Equation (21) instead of (22)

imaginary part of the admittance affects only the value of  $k_r$ . In the interim report prepared under this grant<sup>40</sup>, results are given using Equation (21) which is obtained by applying the trapezoidal rule. The results in Table 1 show a two order of magnitude increase in accuracy for  $y = 0.3$  using Equation (22). The values for  $y = 0.3i$  are the same as those presented in Reference 40 using Equation (21). These cases are not computed employing Equation (22) in order to save on computation time and since no new information can be obtained by doing so.

The accuracy of the computed natural mode shapes is shown in Figure 6. The agreement between the exact and computed eigenmodes for a rigid boundary is to within .01 per cent for interior points sufficiently far removed from the boundary. For a nonzero admittance at the surface, the accuracy is to within two per cent as presented in Figure 7. These results are obtained using the interior analogue of Equation (21) which explains the deterioration in accuracy of the interior points as the boundary is approached. Equation (27) is used in the studies of the rectangle, star, and duct problems and more accurate results are attained.

#### B. Rectangle

The main reason for studying the rectangle is to investigate methods for handling corner points. At these points the normal derivatives are undefined. Since exact solutions can be obtained for the rectangle, the accuracies of these techniques can be assessed.

In this study boundary points were not placed at the corners but were displaced a distance of one-half the integration stepsize from the corner. This method is not the one suggested by Banaugh and Goldsmith<sup>19</sup> in studying the two-dimensional scattering problem. They place the point at the corner

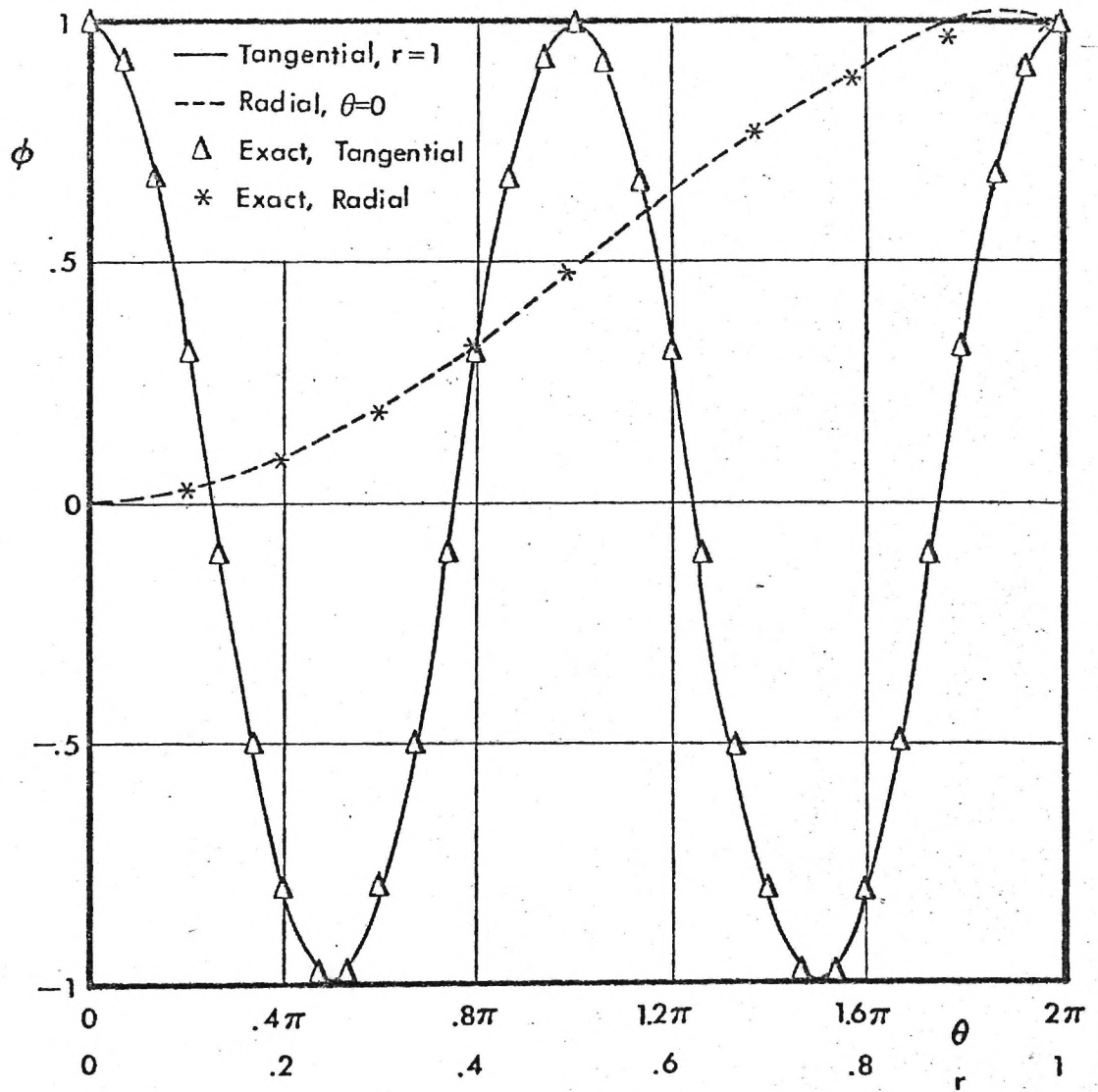


Figure 6. Second Mode for a Circle, Radial and Tangential Potential Values.  $y = 0 + 0i$

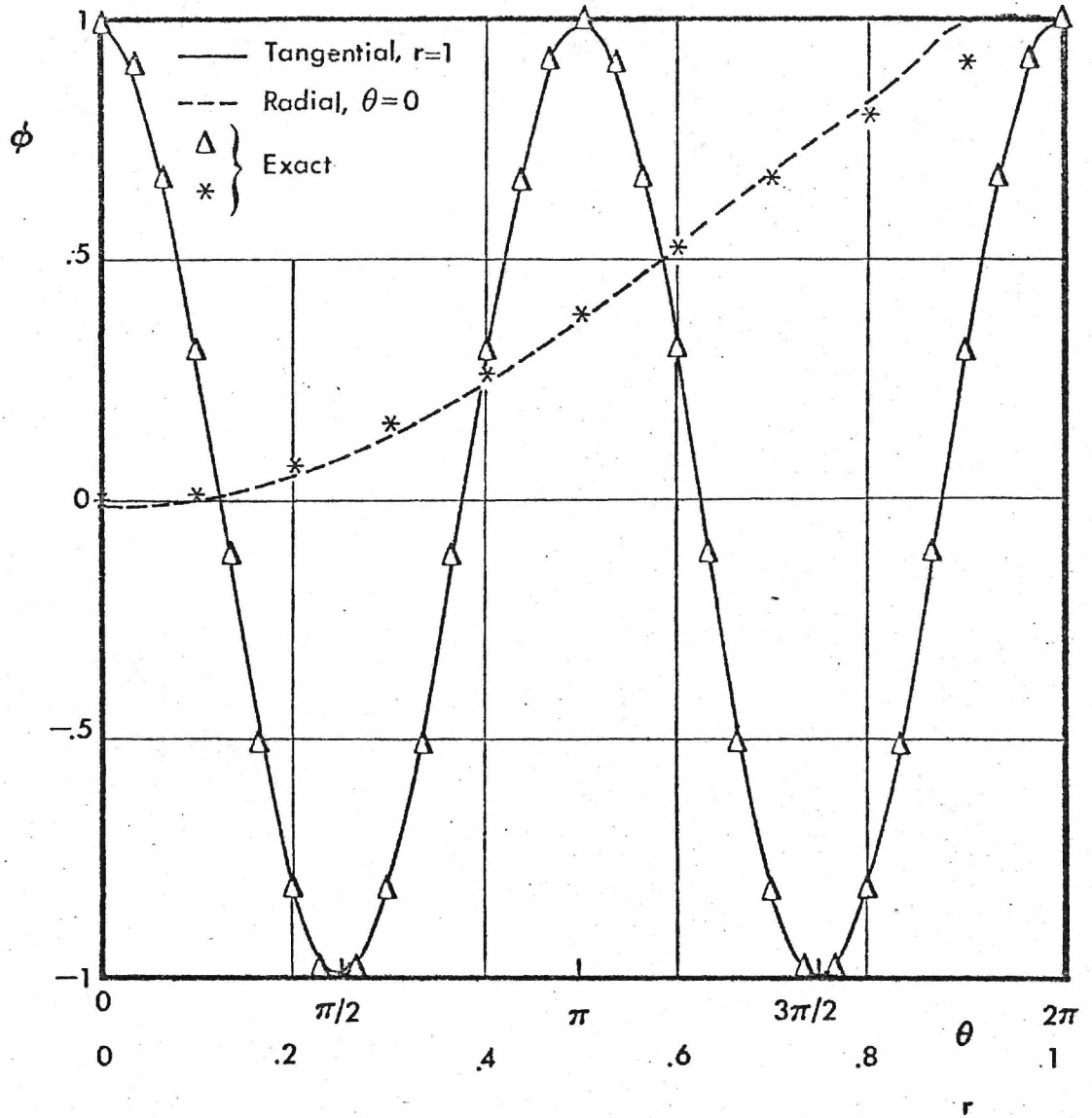


Figure 7. Comparison of Exact and Computed Potentials of a Circle for the Second Mode.  $y = .3i$

and reformulate to account for the fact that a radius vector of arbitrarily small length is turned through an angle  $\theta$  at a corner instead of  $\pi$  for a smooth boundary, where  $\theta$  is the turning angle at the corner point. For the rectangle,  $\theta$  is 90 degrees. Applying their method, the eigenfrequency can be computed to 0.1 or 3 per cent for the first rectangular mode. However, by displacing the point from the corner and using Equation (22), the accuracy is increased by an order of magnitude. The techniques for handling the normal derivatives at the corners is based on the method developed by Banaugh and Goldsmith.

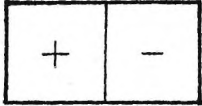
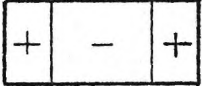
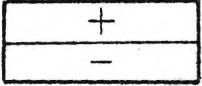
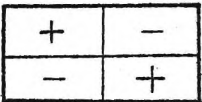
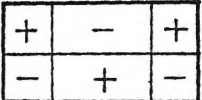
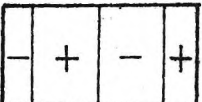
The results are summarized in Table II for 42 points taken on the boundary. As with the circle, the agreement between the exact and numerical values is good for a rigid boundary but deteriorates when a nonzero admittance is introduced. From Table II the agreement is to almost four significant figures in the real part of the eigenfrequency and to within .01 in the imaginary part for a rigid wall. The Gaussian integration techniques developed in Section III and applied to the circle are used for the rectangle to improve the accuracy of the computed eigenfrequencies for a nonzero admittance condition.

The boundary values of the acoustic potential are shown in Figure 8 along lines of constant  $x$  and  $y$ . The effect of an admittance condition on the values along the  $x$  axis is also shown. The agreement between the exact and numerical results is within one-half of a per cent.

In addition to studying the effect of corner points, another phenomenon which occurs for the rectangle is the appearance of two modes existing at one resonant frequency. No reliable analytical formulation can be found for handling this case although Morse and Ingard suggest ways of evaluating

TABLE II.

Resonant Frequencies and Natural Modes of a Rectangle for Different Admittance Values at the ends.

MODE SHAPE		ADMITTANCE VALUE		
		$y = 0 + 0i$	$y = 0.3 + 0i$	$y = 0 + 0.3i$
	COMPUTED	$3.1432 - 0.0015i$	$3.150 + 0.6199i$	$2.558 + 0.0019i$
	EXACT	3.1416	$3.142 + 0.6190i$	2.559
 	COMPUTED	$6.2877 - 0.0041i$	$6.302 + 0.6156i$	$5.886 - 0.0024i$
	EXACT	6.2832	$6.283 + 0.6190i$	5.884
	COMPUTED	$7.0312 - 0.0098i$	$7.146 + 0.5880i$	$6.333 - 0.0066i$
	EXACT	7.0248	Not Computed	6.283
	COMPUTED	$8.8929 - 0.0184i$	$8.934 + 0.6099i$	$8.303 - 0.0111i$
	EXACT	8.8858	Not Computed	8.299
	COMPUTED	$9.4329 - 0.0074i$	$9.456 + 0.6106i$	$8.847 + 0.0069i$
	EXACT	9.4248	$9.425 + 0.6190i$	8.842



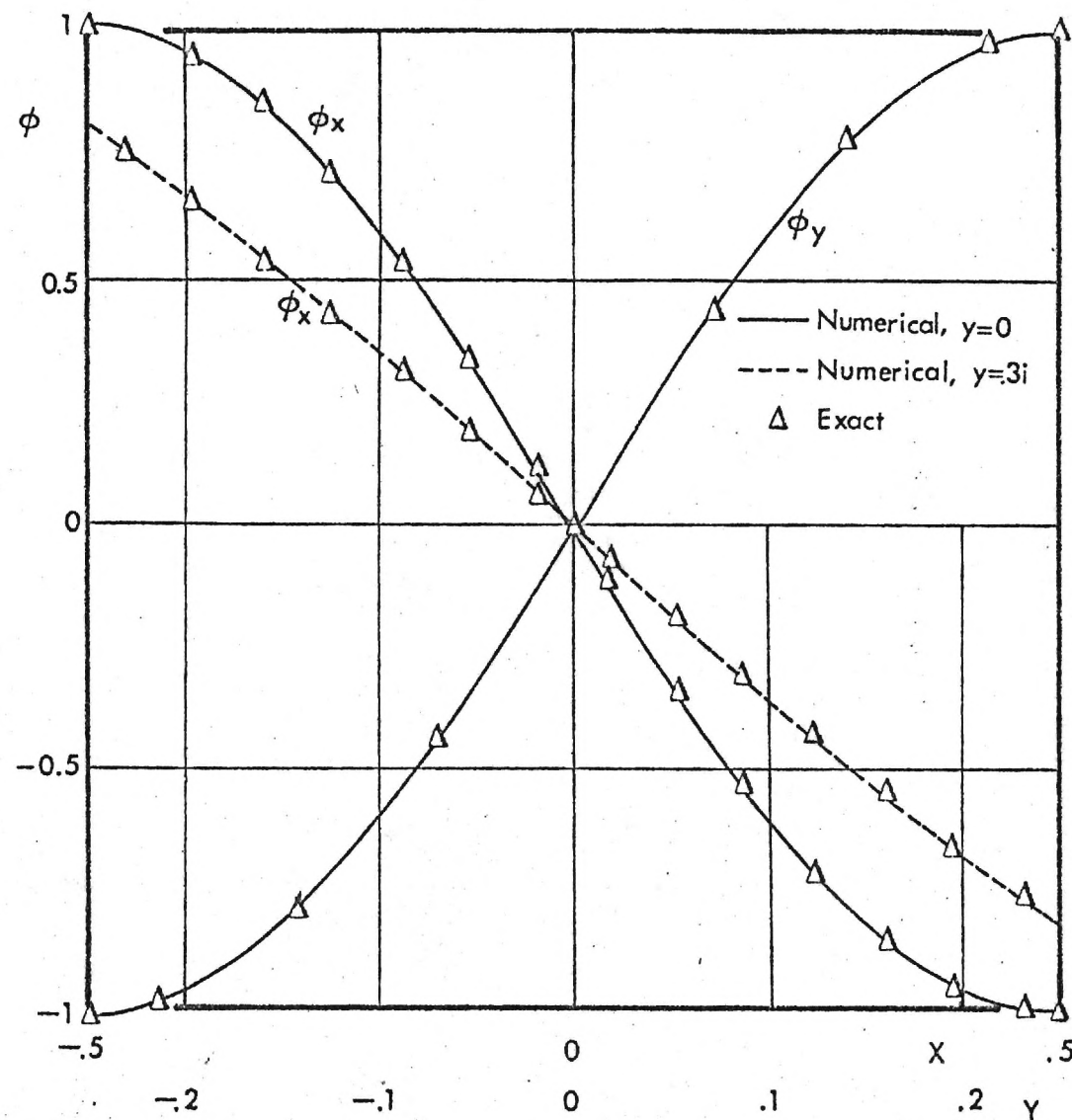


Figure 8. Comparison of the Numerical and Exact Surface Potential Values of a Rectangle for Two Admittance Conditions.

these modes<sup>3</sup>. In practice, it is possible to find both of these modes by taking sufficiently fine step sizes in  $k$ . The frequencies of the two modes is not identically the same when numerical integration is used. Also, when an admittance condition is applied, the eigenfrequencies of the modes occur at different values.

The comparison between the computed and exact interior fields taken along the centerline of the rectangle for the first mode is presented in Figure 9. The results compare to within one per cent even for points a distance of only half of an integration step size from the boundary. This result demonstrates the accuracy which is achieved by using Equation (27) instead of the interior analogue of Equation (21).

### C. Star

In studying the star-shaped boundary, the applicability of the integral relations to a complicated geometry for which separation of variables does not apply can be assessed. The first nine eigenfrequencies and natural modes for the star are presented in Figure 10 for a rigid wall with forty-eight points taken on the surface. These results are also reported in the interim report<sup>40</sup>. The most unique feature of the acoustic field for the star is the appearance of nodal points at some of the resonant modes. In the circle and rectangle nodal lines only were present and followed one of the separable coordinates of the boundary. With the star both nodal lines and points can occur which is in qualitative agreement with experimental observations. Isometric views of the pressure fields for the third and fifth modes are shown in Figures 11 and 12.

Another unique feature of the modes of the star is the phase between

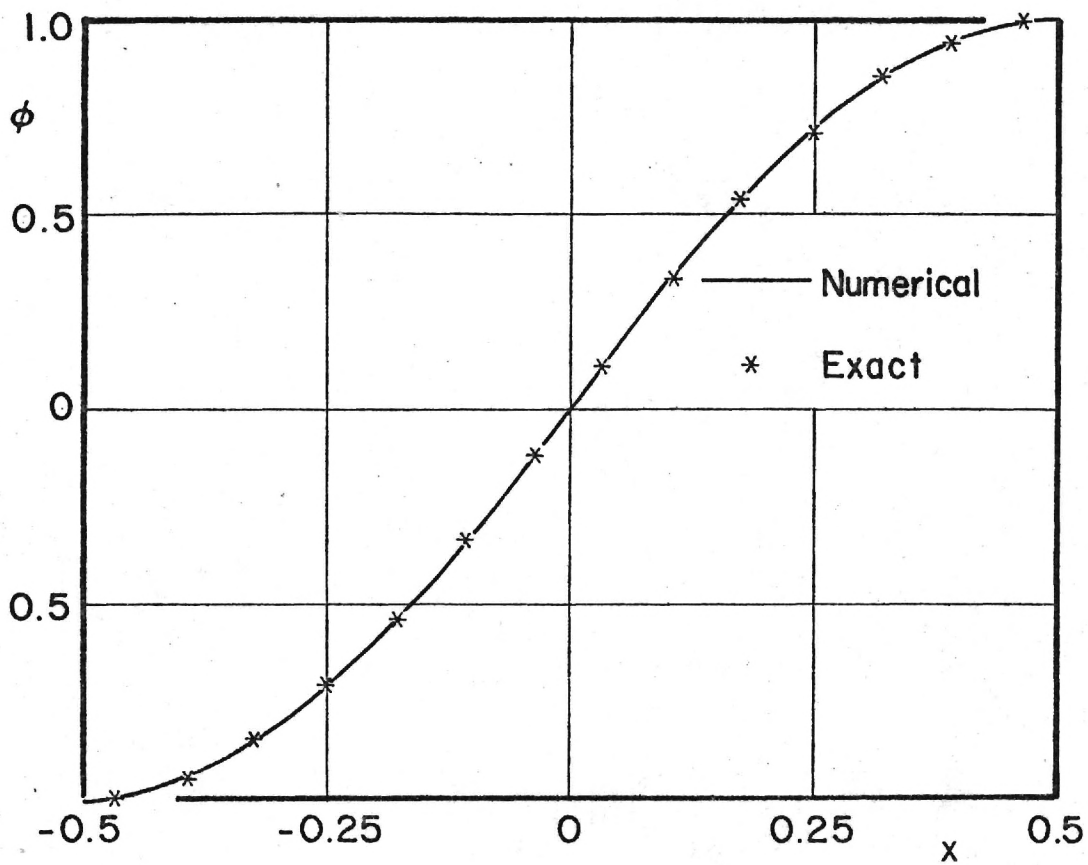


Figure 9. Comparison of the Exact and Numerical Internal Potential Values along the Centerline of the Rectangle.

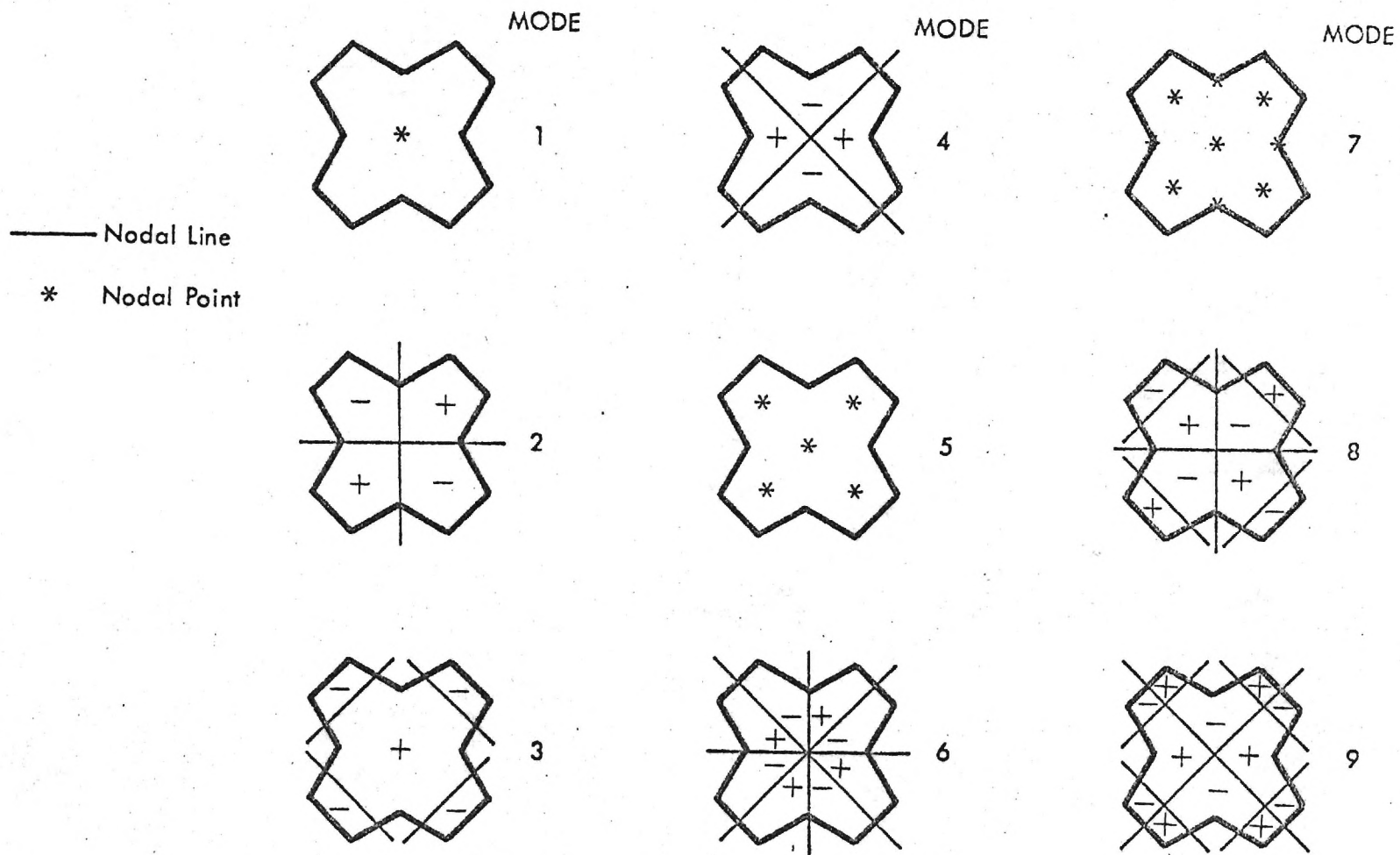


Figure 10. Nodal Points and Lines for the First Nine Modes of the Star.

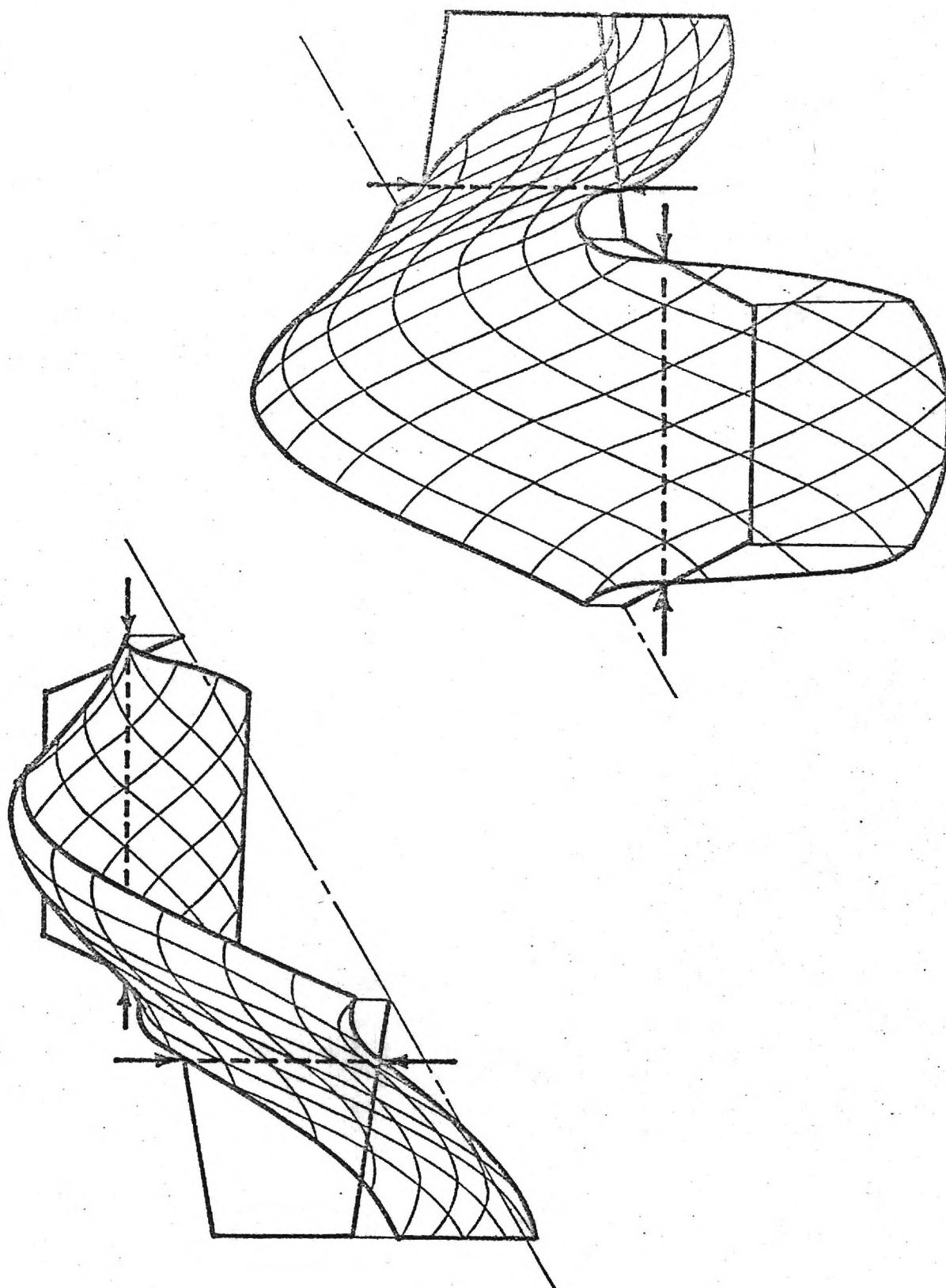


Figure 11. Altitude Chart of the Pressure Distribution for the Third Mode of the Star. Arrows Point to the Nodal Lines.

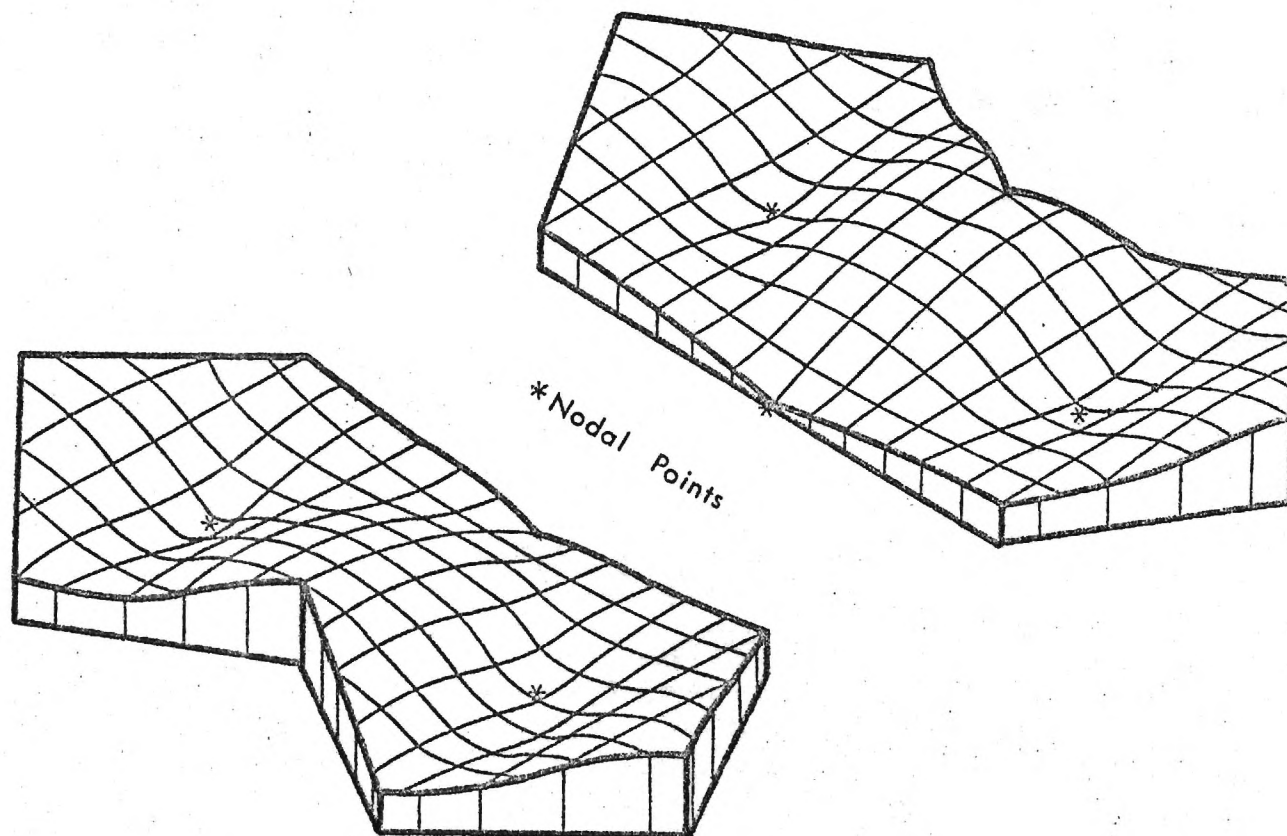


Figure 12. Altitude Chart of the Pressure Distribution for the Fifth Mode of the Star.



the pressure oscillations at two interior points. For the modes containing nodal lines, the pressure oscillations are either in phase or 180 degrees out of phase at every point. This result was also obtained for the circle and rectangle. However, for the modes containing nodal points the phase varies continuously along lines parallel to the boundary.

The numerical technique is also applied to three and four quadrant star configurations typical of the cross section of a solid propellant combustor at various times during a burn. Forty-eight points are taken on the boundary and computation times range from 60 to 75 seconds per mode. The resulting modes of a four quadrant star are presented in Figure 13. This figure shows the first three modes for four geometries which occur at different times during burning. The dimensions in these figures have been normalized, so the shapes do not appear to increase in size as the burn progresses.

In Figure 14, the corresponding results are presented for a star with three quadrants. Here, only the first and third modes are shown. The second mode, which is not shown, appears to have more than one nodal point and a contour plot is needed to investigate its shape.

In Figures 15 and 16, the variation in the real and the imaginary parts of  $k$  are plotted against burn time. A constant admittance of  $-0.05$  is assumed throughout the burn. This negative admittance value indicates driving and is typical of a solid propellant combustion process.

Two effects are evident. First, the frequency  $k_r$  changes significantly with time because of the increasing size and changing geometry of the combustor. Second, the negative values of  $k_i$  indicate that the oscillations grow with time. The figures show that the propellant is most likely to be

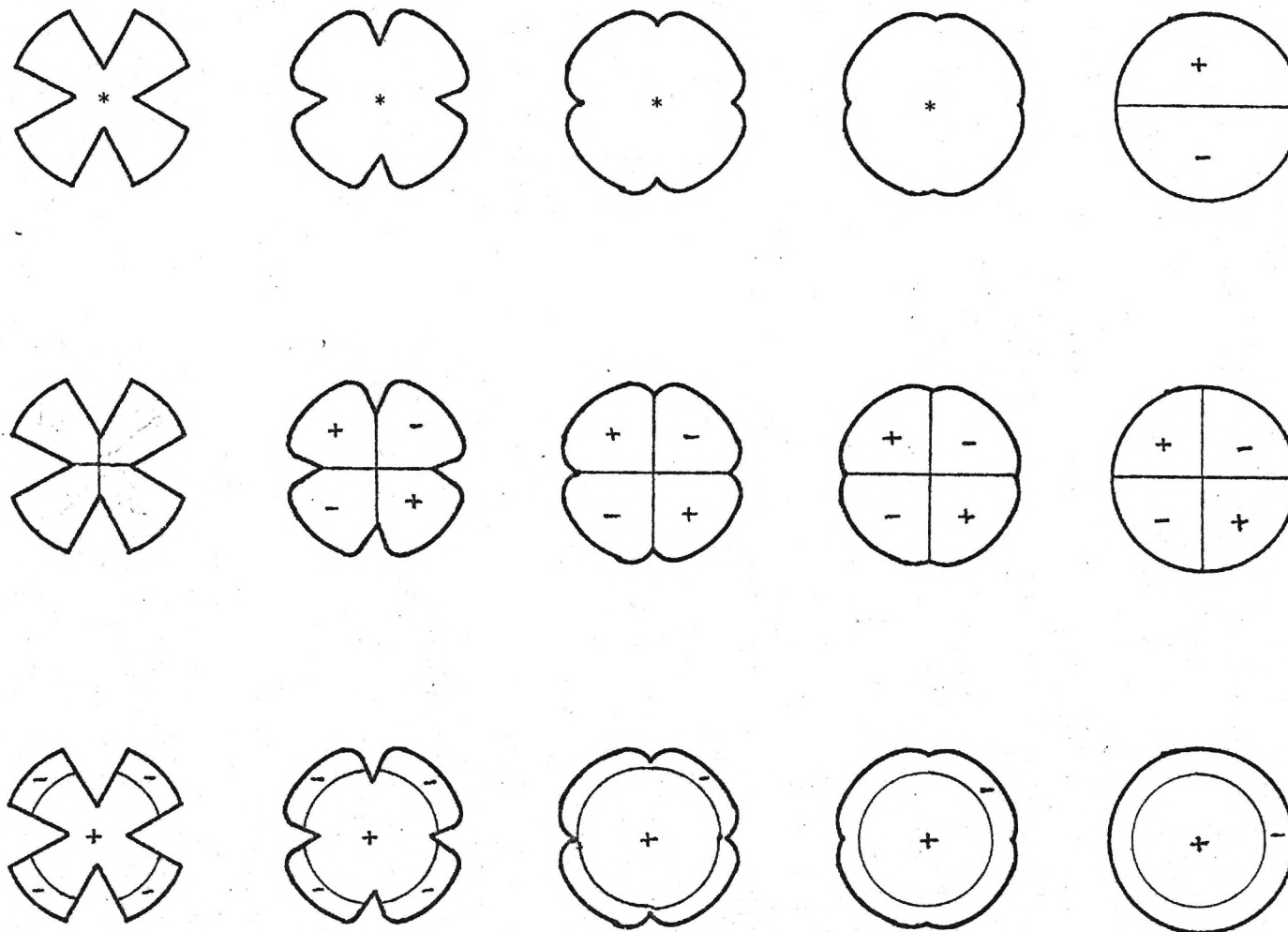


Figure 13. First Three Eigenmodes of a Four-Quadrant Star During Burning

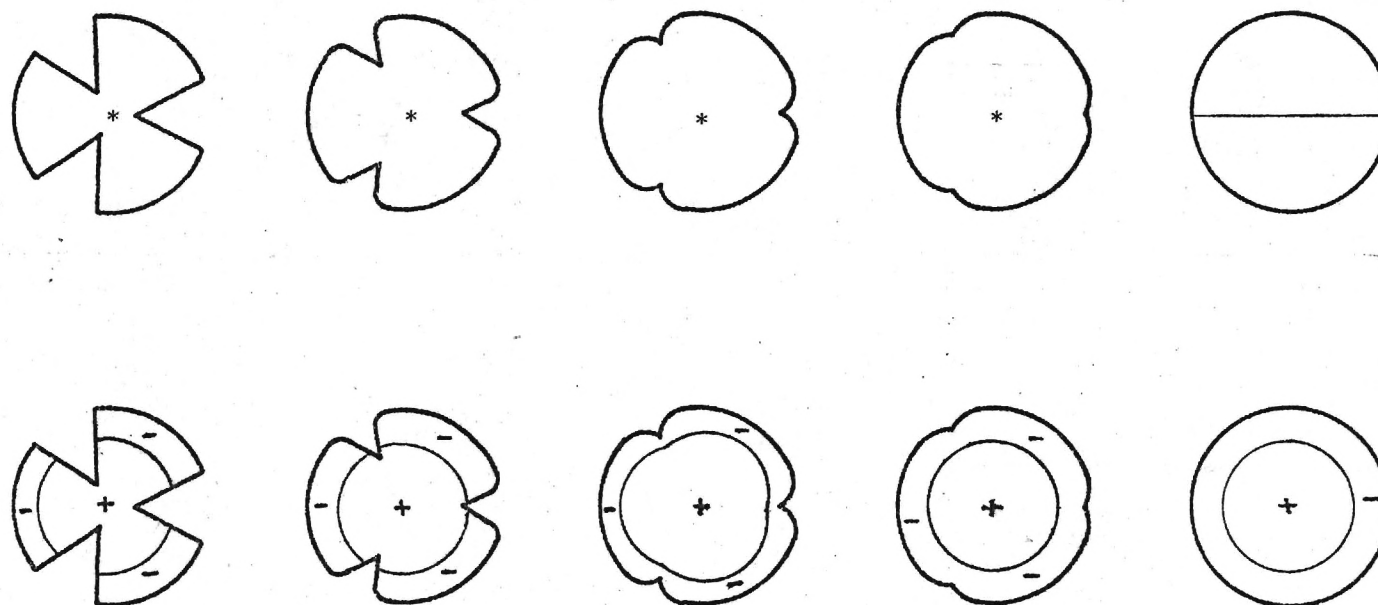


Figure 14. Eigenmodes of a Three-Quadrant Star during Burning

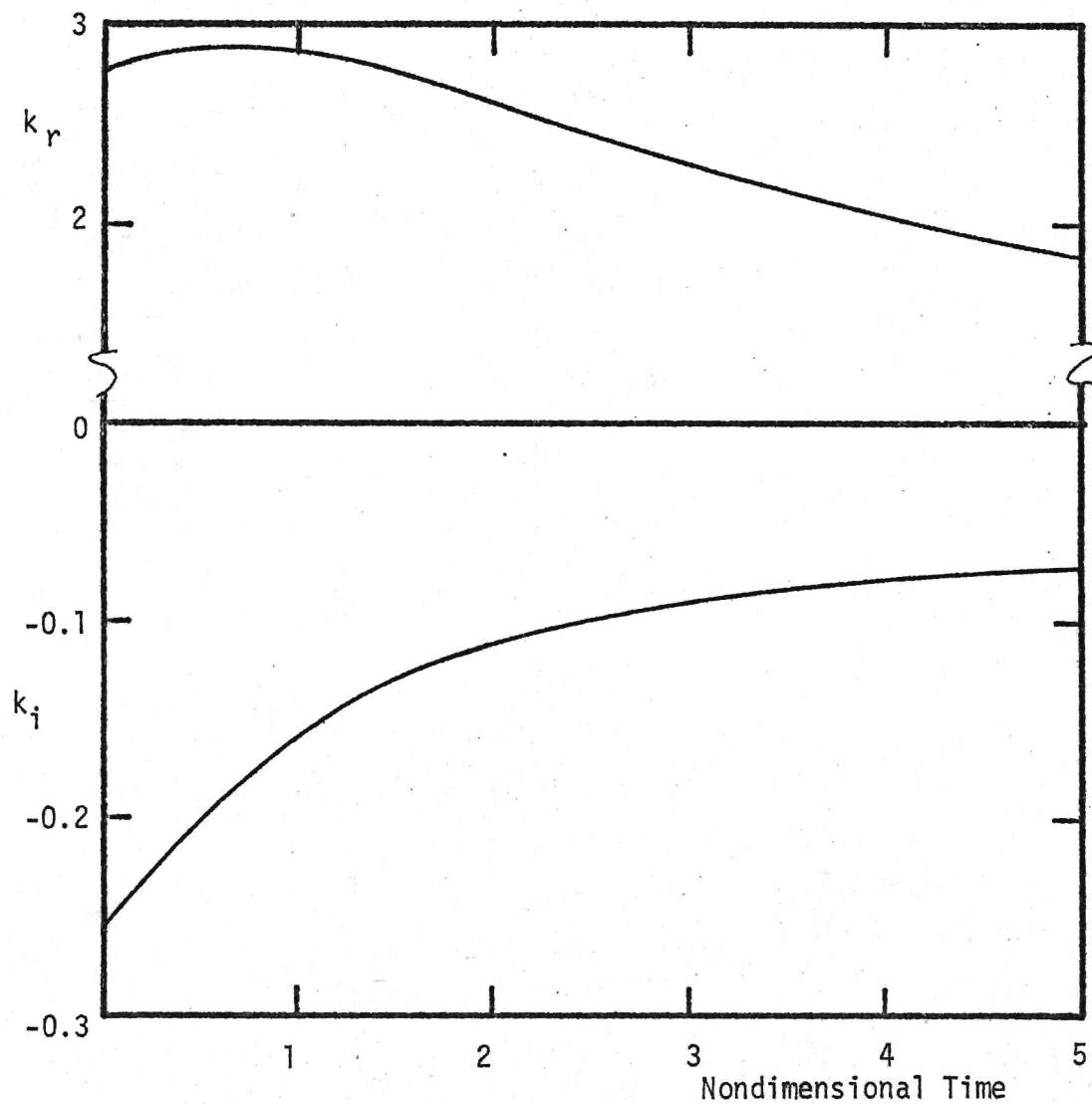


Figure 15 Change in the Eigenfrequency during Burning, Four-Quadrant Star, First Mode

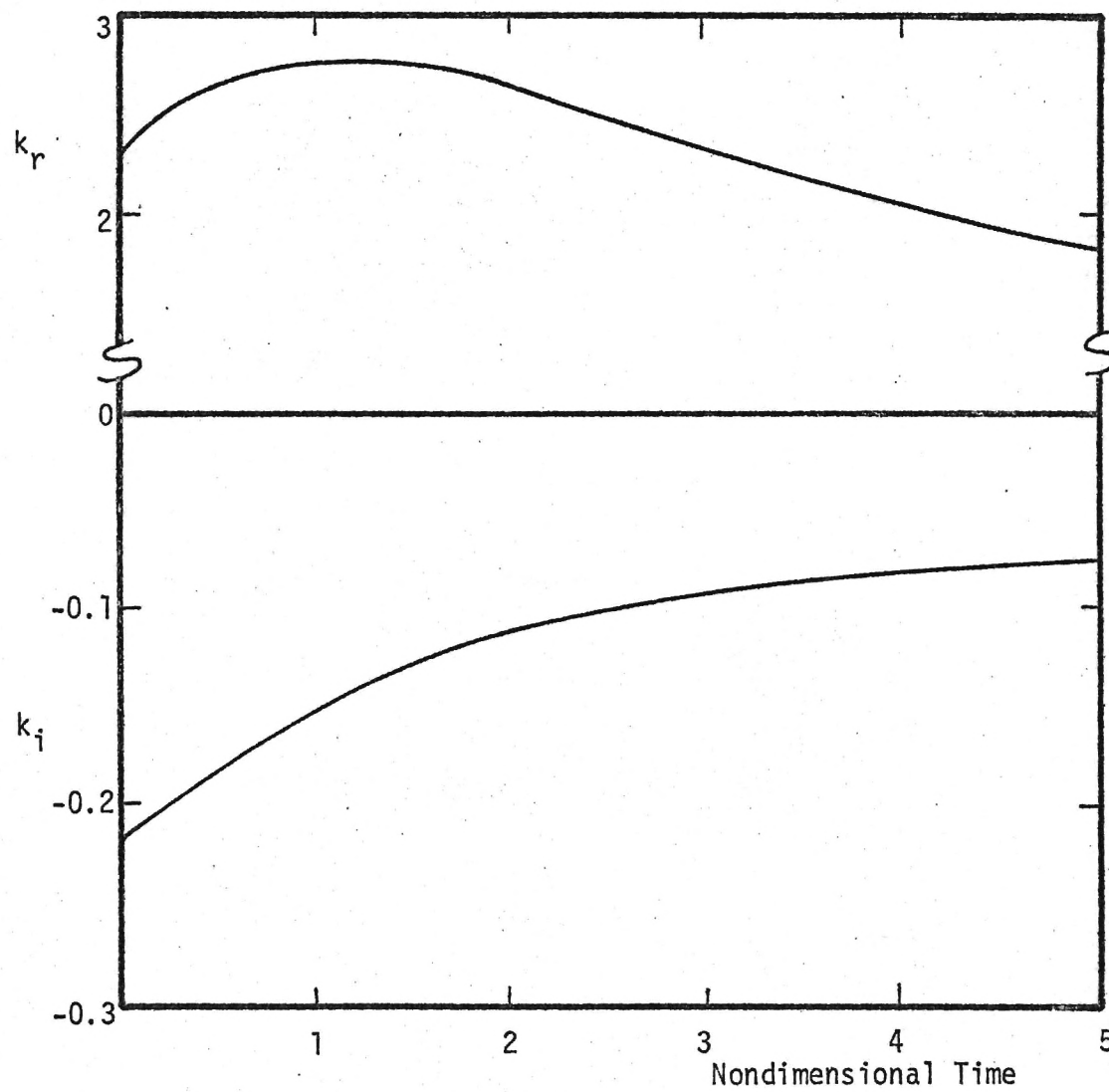


Figure 16. Change in the Eigenfrequency during Burning, Three-Quadran Star, First Mode

unstable initially than during later times in the burn. These results indicate the applicability of this research to practical problems.

#### D. Duct with a Right Angle Bend

The last two-dimensional problem investigated in this research is that of a duct with a right-angle bend shown in Figure 17. The reasons for studying this configuration are: (1) to investigate a nonuniform surface admittance, (2) to include a sound source in the integral formulation, and (3) compare the results obtained by the integral technique with the finite difference solutions of Reference 13.

The results obtained using this configuration are presented in Figures 18 and 19 and are compared with the solutions obtained using the finite difference method. Although the results using the integral approach are in qualitative agreement with the finite difference solution, quantitative agreement is lacking. The same number of boundary points are taken in both cases. Doubling the number of subintervals using Equation (22) modified for a sound source does not improve the agreement between the two sets of data. However, it does show that the results of the integral formulation are self-consistent.

An experiment is currently being fabricated to check these results and should clarify the discrepancy between these two methods.

#### E. Other Studies

The two-dimensional studies have been carried out by the principal investigator. In addition, a graduate research assistant, William L. Meyer, has been conducting studies on three-dimensional problems. Preliminary results for the radiation sound field from a sphere with a radiating piston compare with exact results to within 4% for 120 surface points. The assoc-



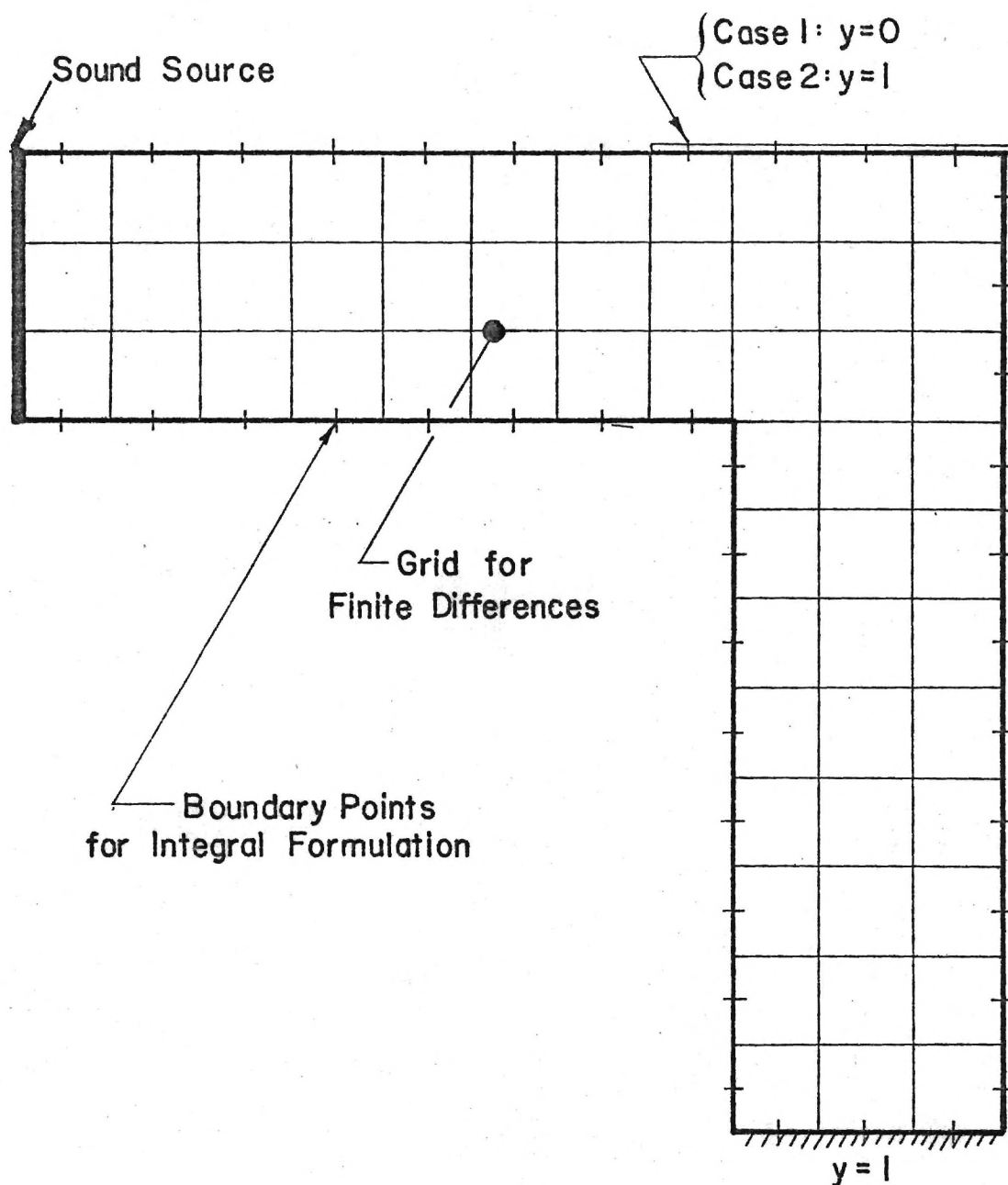


Figure 17. Location of the Discrete Points, Nonzero Admittance Boundaries, and the Sound Source for the Duct with a Right Angle Bend.

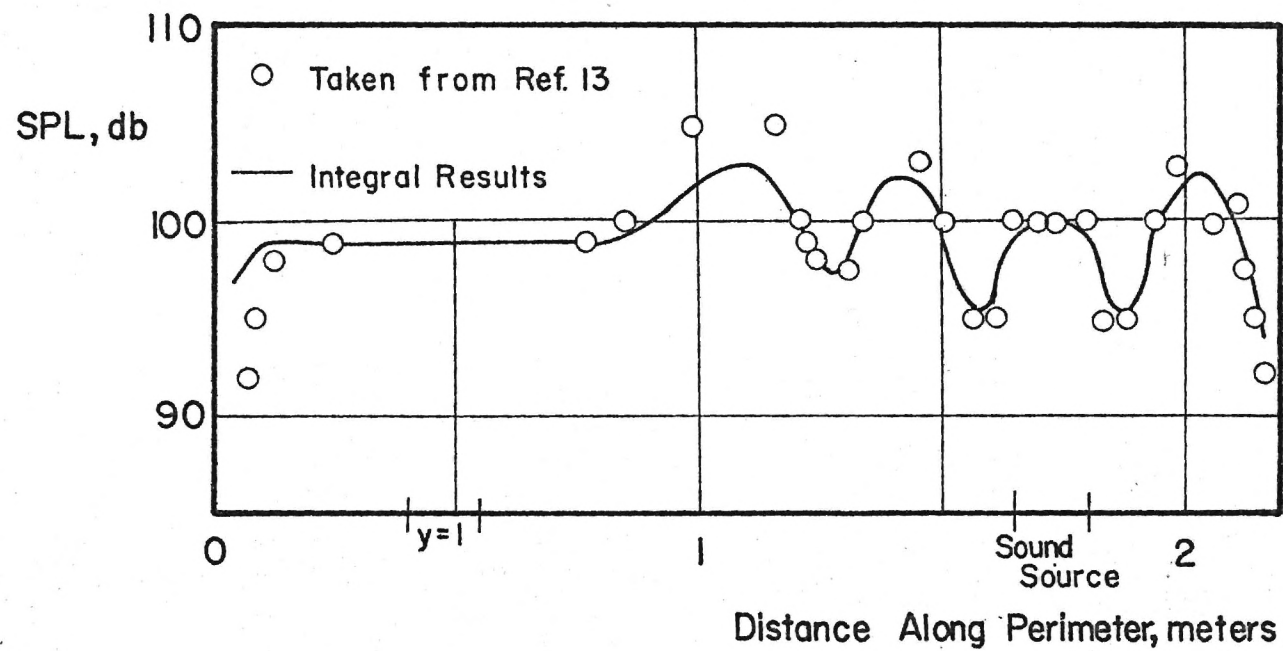


Figure 18. Comparison of Numerical Results for a Duct with a Right Angle Bend Using the Integral and Finite Difference Approaches, Case 1.

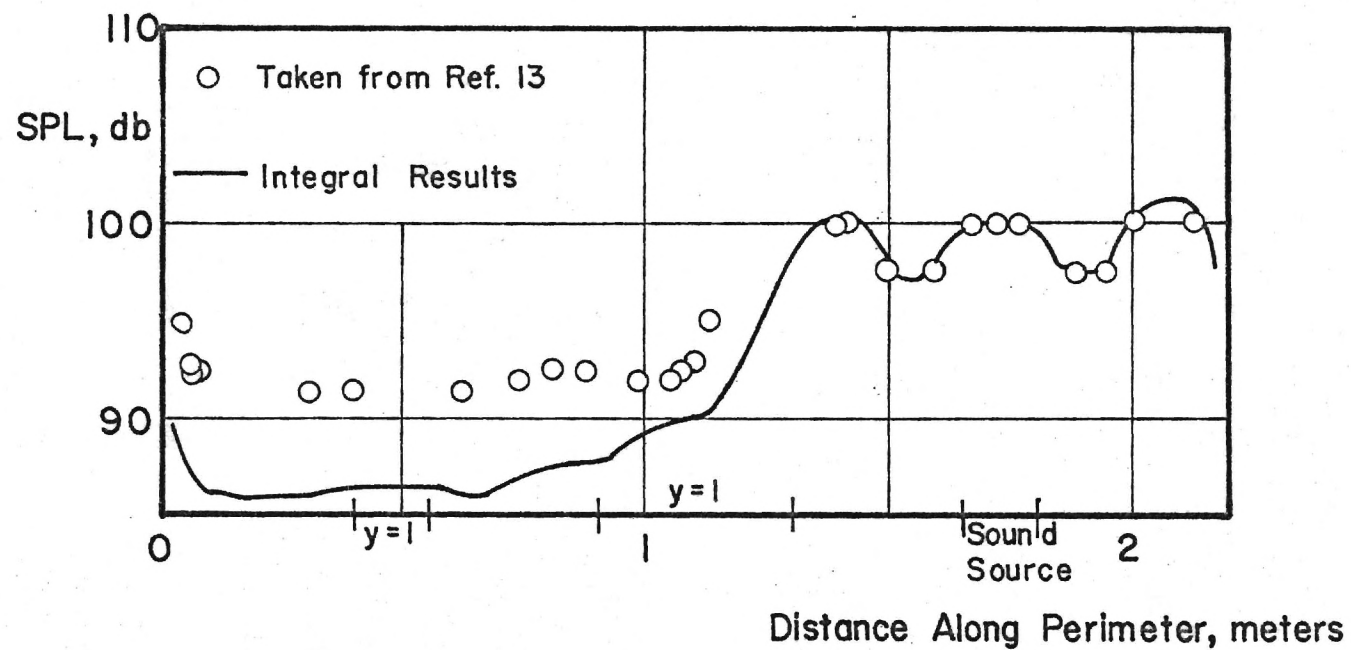


Figure 19. Comparison of Numerical Results for a Duct with a Right Angle Bend Using the Integral and Finite Difference Approaches, Case 2.

iated computation time on a UNIVAC 1108 is about two minutes to solve for the sound pattern. In a previous study by Chen and Schweikert<sup>6</sup>, for 80 points the error between the numerical and exact results was 18% and computation times on a comparable computer were about 105 minutes.

Because of the similarity of the integral equations for solving internal and external sound fields, large errors in the numerical solution of external problems (radiation and scattering) occur at frequencies close to the internal eigenvalues of the radiating body. After applying several numerical techniques for avoiding this problem, Meyer has developed an efficient method for obtaining reliable results even at the eigenfrequencies. A survey paper is planned for publication concerning this work.

#### F. Summary of Results

Using the integral formulation, results are presented for a circle, rectangle, star and a duct with a right angle bend. The resonant frequencies and natural modes for the circle and rectangle agree well with exact solutions using Equations (22) and (27). Equation (21) gives good results for a rigid boundary, but leads to inaccuracies when an admittance condition is introduced. For a star configuration, the appearance of nodal points in the natural mode shapes is predicted which is in qualitative agreement with experimental observations. For a duct with a right angle bend, the applicability of the integral formulation to problems involving general boundary conditions is demonstrated. The results are in qualitative agreement with finite difference solutions but quantitative agreement is lacking. Experiments will be performed to resolve this discrepancy.

## V. CONCLUSIONS, RECOMMENDATIONS, AND POSSIBLE FUTURE STUDIES

Based on the analytical studies presented in Section III and the numerical results of Section IV, the following conclusions and recommendations are made.

- (1) For problems involving rigid boundaries, the trapezoidal rule used in previous studies can be used to discretize the integral equations and obtain good results. However, for a nonzero admittance condition at the surface, Equation (22) should be used employing Gaussian quadrature to evaluate the integrals involving the Hankel functions over each subinterval. Equation (27) should be used for both zero and nonzero admittances to determine interior points.
- (2) For general boundary shapes, the following procedure should be used to determine the geometric parameters appearing in Equation (22). First, divide the boundary line into  $N$  subintervals. Then, specify the  $x$  and  $y$  coordinates and the normal vector at the midpoint of each subinterval. Finally, specify the length of each line segment of the subintervals. Once these parameters are known,  $r$  and  $\partial r / \partial n$  can be obtained from Equations (23) and (24). For simple geometries, parametric equations can be used but are not necessary for accurate results. For corners, the best results are achieved by placing two points on both sides of the corner. Placing the point at the corner and reformulating the integral equations as suggested by Banaugh and Goldsmith, does not yield results as accurate as those ob-

tained using the procedure developed in this study.

- (3) To determine the resonant frequencies of a particular geometry, the procedure developed in Section III is suggested. Since this study is the first undertaken to determine the resonant frequencies for general admittances using the integral approach, more efficient techniques can probably be developed. However, the one presented in Section III yields accurate results for the geometries considered in this investigation.
- (4) The results for the circle and rectangle show that the integral technique is very accurate in determining resonant frequencies and natural mode shapes. Its application to the star configuration demonstrates its usefulness in studying the acoustics of complicated shapes. For the duct with a right-angle bend, the integral approach is shown to be applicable to nonuniform boundary conditions involving sound sources.

The results obtained for the two-dimensional problem demonstrate that the integral technique is an accurate and rapid means for determining the acoustic properties of two-dimensional ducts with complicated shapes. Extensions of this formulation can be made to cover a wide range of acoustic problems. These include the following:

- (1) Since the numerical techniques are directly applicable to two-dimensional radiation and scattering problems, studies in this area can be made to improve the accuracy of the



predictions obtained to date. The major problem would be to investigate techniques for minimizing the errors which occur in the sound field when the frequency is close to an eigenfrequency of the particular geometry considered. Techniques currently in use require a severe penalty in computer time and complexity. A technique has been developed by W. L. Meyer which minimizes this problem in three dimensions and has been shown to be easy to apply and efficient with respect to computer time. A two-dimensional analogue could be formulated and applied.

- (2) The numerical techniques developed for the two-dimensional problem can also be used in axisymmetric radiation, scattering, and duct problems. The major change would be the use of a different Green's function<sup>18</sup>. The integral equations involved, however, would retain their essential two-dimensional character. The axisymmetric formulation is applicable to antenna scattering, radiation from ducts (such as the aircraft inlet noise problem), and waveguide theory. Considerable work is needed in these areas.
- (3) Three-dimensional problems have also been investigated at no cost to this grant. These include the radiation from a sphere, computation of the internal eigenfrequencies of a cylinder, and investigations of the breakdown of the integral formulation for external problems at the corresponding eigenfrequencies of the geometry under consideration. Major results include development of more effi-

cient numerical methods which reduce computation times by two orders of magnitude over the methods currently in use and an efficient, rapid technique for computing external fields at eigenfrequencies. These techniques could be applied to a broad range of acoustic and electromagnetic problems.

## APPENDIX A

### BRIEF DESCRIPTION OF COMPUTER PROGRAMS

## APPENDIX A

To conduct these investigations, the computing facilities of the Georgia Institute of Technology are employed. The available hardware and software applicable to this research will be briefly described.

### A. Hardware

To perform the necessary computations, a UNIVAC 1108 computer was used. This computer has a core storage capacity of 65 K which is sufficient for the two-dimensional acoustic wave propagation studies. During the course of this investigation, a new computer was acquired from CDC called the CYBER 70. This resulted in a loss of about four months to this project for program modification. In addition to converting to a new operating system, the programs had to be changed from FORTRAN V used on the 1108 to extended FORTRAN IV used on the CYBER 70. However, the programs could run two to five times faster on the CYBER 70 than on the UNIVAC 1108. Also the CYBER has a 90 K storage capacity which is 35 K more than the UNIVAC.

### B. Software

To compute the acoustic field and resonant frequencies, the coefficients of the discretized integral equations are determined first. This involves the calculation of  $r$  and the normal derivative  $\partial/\partial n$  at every point. These parameters can be found from the parametric equations which describe the surface contour or by specifying the coordinates and normal vector at each point. The Hankel functions with complex arguments which also appear in the expressions for the coefficients were first calculated using a computer program developed by the principal investigator and later by using a more efficient routine. The accuracy of the resulting values has been veri-

fied over a wide range of order and arguments.

Once the coefficients have been determined, the set of complex linear algebraic equations and the complex determinants are solved using Gauss-Jordan reduction. The necessary computer program is available in the library routines of the computers. However, since the coefficient matrix is diagonally dominant, a routine is used without pivotal condensation to minimize time.

A general flow chart for the computer programs used in research is given in Figure A-1. To minimize the time required for program modification in changing the surface geometry or boundary conditions, the computer program is divided into several subroutines. Rather than modifying parts of the entire program, only the affected subroutine need be changed.

The subroutine SHAPE gives the x and y coordinates of the surface contour, the normal vector components, the line segment lengths, and the admittance of the surface at each point. This information is returned to subroutine BDRY where the basic geometric properties, integration distances and boundary conditions are determined. These data are sent to BEGIN which computes the value of the resonant frequency. This value is used by subroutine FREQ, to determine the eigenvalues using the quadratic interpolation method. The boundary values of the potential functions are then computed in the subroutine BVALUE by the Gauss-Jordan reduction scheme and used to compute the interior values of the potential in subroutine MODE. In the subroutines HANKEL and COEFF, the Hankel functions and coefficients are computed.

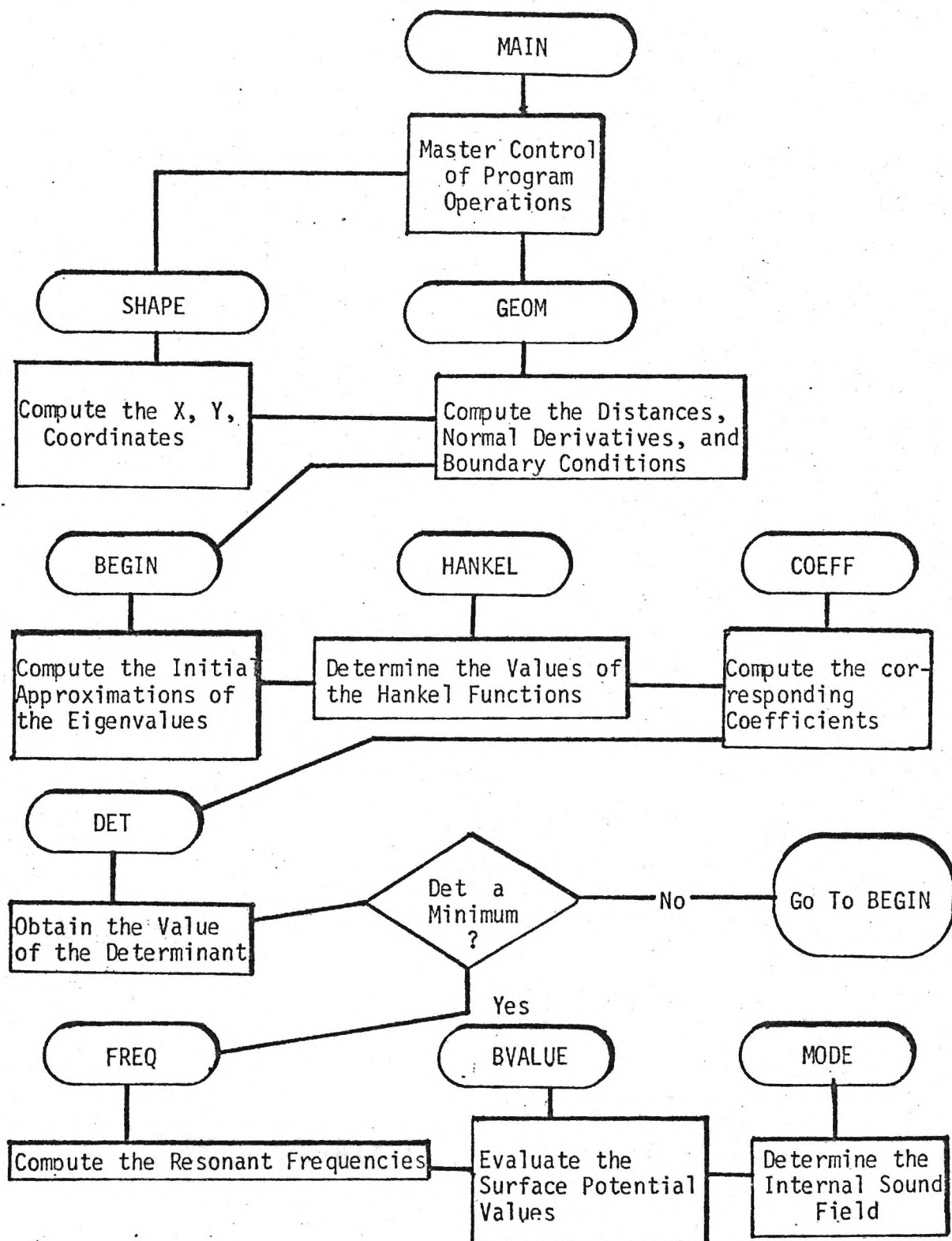


Figure A-1. Flowchart of the Computer Program



## REFERENCES

1. Morse, P. M. and Feshbach, H., Methods of Theoretical Physics, Parts I and II, McGraw-Hill, New York, 1953.
2. Weinberger, H. F., A First Course in Partial Differential Equations, Blaisdell Publishing Company, Waltham, MA., 1965.
3. Morse, P. M. and Ingard, K. U., Theoretical Acoustics, McGraw-Hill, New York, 1969, Chapter 9.
4. Skudrzyk, E., The Foundations of Acoustics, Springer-Verlag, Wien, Austria, 1971, Chapters 22 and 23.
5. Mitchell, C. E., Espander, W. R., and Baer, M. R., "Determination of Decay Coefficients for Combustors with Acoustic Absorbers", NASA CR 120836, January 1972.
6. Oberg, C. L., "Improved Design Techniques for Acoustic Liners", Report No. RR-68-5, Rocketdyne, Canoga Park, CA, May 1968.
7. Oberg, C. L., Wong, T. L., and Schmeltzer, R. A., "Analysis of the Acoustic Behavior of the Baffled Combustion Chambers", NASA CR 72625, January 1970.
8. Doak, P. E., "Excitation, Transmission and Radiation of Sound from Source Distributions in Hard-Walled Ducts of Finite Length (I): The Effects of Duct Cross-Section Geometry and Source Distribution Space-Time Pattern, (II): The Effects of Duct Length", Journal of Sound and Vibration, Vol. 31, No. 1, pp 1-72, and Vol. 31, No. 2, pp. 137-174, 1973.
9. Lansing, D. L. and Zorumski, W. E., "Effects of Wall Admittance Changes on Duct Transmission and Radiation of Sound", Journal of Sound and Vibration, Vol. 27, No. 1, 1973, pp. 85-100.
10. Wynne, G. A. and Plumbee, H. E., "Calculation of Eigenvalues of the Finite Difference Equations Describing Sound Propagation in a Duct Carrying Sheared Flow", Paper presented at the 79th Meeting of the Acoustical Society of America at Atlantic City, New Jersey, April 21, 1970.
11. Baumeister, K. J., "Application of Finite Difference Techniques to Noise Propagation in Jet Engines", NASA TMX-68621, November 1973.
12. Baumeister, K. J. and Rice, E. J., "A Difference Theory for Noise Propagation in an Acoustically Lined Duct with Mean Flow", AIAA Paper No. 73-1007, October 1973.
13. Alfredson, R. J., "A Note on the Use of the Finite Difference Method for Predicting Steady State Sound Fields", Acustica, Vol. 28, No. 5, 1973, pp. 296-301.

14. Cantin, G., "Three-Dimensional Finite Element Studies, Part One: Service Routines", NPS-59C172121A, Naval Postgraduate School, Monterey, CA, December 1972.
15. Chen, L. H. and Schweikert, D. G., "Sound Radiation from an Arbitrary Body", Journal of the Acoustical Society of America, Vol. 35, No. 10, October 1963, pp. 1626-1632.
16. Chen, L. H., "A Matrix Method of Analysis of Structure-Fluid Interaction Problems", ASME Paper No. 61-WA-220, August 1961.
17. Chertock, G., "Sound from Vibrating Surfaces", Journal of the Acoustical Society of America, Vol. 36, No. 7, July 1964, pp. 1305-1313.
18. Copley, L. G., "Integral Equation Method for Radiation from Vibrating Bodies", Journal of the Acoustical Society of America, Vol. 4, No. 4, April 1967, pp. 807-816.
19. Banaugh, R. P. and Goldsmith, W., "Diffraction of Steady Acoustic Waves by Surfaces of Arbitrary Shape", Journal of the Acoustical Society of America, Vol. 35, No. 10, October 1963, pp. 1590-1601.
20. Banaugh, R. P. and Goldsmith, W., "Diffraction of Steady Elastic Waves by Surfaces of Arbitrary Shape", ASME Paper No. 63-WA-36, November 1963.
21. Mitzner, K. M., "Numerical Solution for Transient Scattering from a Hard Surface of Arbitrary Shape-Retarded Potential Technique", Journal of the Acoustical Society of America, Vol. 42, No. 2, February 1967, pp. 391-397.
22. Shaw, R. P., "Scattering of Plane Acoustic Pulses by an Infinite Plane with a General First-Order Boundary Condition", Journal of Applied Mechanics, September 1967, pp. 770-772.
23. Liu, H. K. and Martenson, A. J., "Optimum Lining Configurations", in Basic Aerodynamic Noise Research, NASA SP-207, July 1969, pp. 425-434.
24. Zinn, B. T. and Gaylord, C. G., Unpublished notes and "An Analytical Investigation of Acoustic Modes of Two and Three Dimensional Solid Rocket Motors", a Thesis Proposal by C. G. Gaylord, School of A. E.
25. Tai, G. C. and Shaw, R. P., "Eigenvalues and Eigenmodes for the Homogeneous Helmholtz Equation for Arbitrary Domains", Report No. 90, Dept. of E. S., State University of New York at Buffalo, August 1973.
26. Kellogg, O. D., Foundations of Potential Theory, Dover Publications, New York, 1953, Chapter VI.
27. Webster, A. G., The Dynamics of Particles, Dover Publications, New York, 1959, Chapter VIII.
28. Baker, B. B. and Copson, E. T., The Mathematical Theory of Huygens' Principle, Oxford at the Clarendon Press, 1950, Chapter I.

29. Burton, A. J., "The Solution of Helmholtz's Equation in Exterior Domains Using Integral Equations", NPL Report NAC 30, National Physical Laboratory, Teddington, Middlesex, January 1973.
30. Strutt, J. W. (Lord Rayleigh), The Theory of Sound, Vol. II, Dover Publications, New York, 1945, Chapter 16.
31. Ingard, K. U., "On the Theory and Design of Acoustic Resonators", Journal of the Acoustical Society of America, Vol. 25, No. 6, November 1953, pp. 1037-1061.
32. Crocco, L. and Sirignano, W. A., "Behavior of Supercritical Nozzles under Three-Dimensional Oscillatory Conditions", AGARDograph 117, Butterworth Publications, London, 1967.
33. Scott, R. A., "An Apparatus for Accurate Measurement of the Acoustic Impedance of Sound Absorbing Materials", Proceedings of the Physical Society, Vol. 58, 1946, p. 253.
34. Zinn, B. T., Bell, W. A., and Daniel B. R., "Experimental Determination of Three-Dimensional Liquid Rocket Nozzle Admittances", AIAA Journal, Vol. 11, No. 3, March 1973, pp. 267-272.
35. T-Burner Manual, Chemical Propulsion Information Agency, CPIA Publication No. 191, November 1969.
36. Crocco, L. and Cheng, S. I., "Theory of Combustion Instability in Liquid Propellant Rocket Motors", AGARDograph 8, Butterworth Publications, London, 1956.
37. Culick, F. E. C., "A Review of Calculations for Unsteady Burning of a Solid Propellant", AIAA Journal, Vol. 6, No. 12, December 1968, pp. 2241-2255.
38. Conte, S. D., Elementary Numerical Analysis, McGraw-Hill, St. Louis, 1965, Chapters 2 and 5.
39. Abramowitz, M. and Stegun, I. A., Handbook of Mathematical Functions, NBS AMS No. 55, May 1968.
40. Bell, W. A., "Resonant Frequencies and Natural Modes of Arbitrarily Shaped Ducts", Annual Report for the Period April 1, 1974 to April 1, 1975 for NSF Research Initiation Grant GK-42159, Georgia Institute of Technology, Atlanta, GA.
41. Jones, D. S., "Integral Equations for the Exterior Acoustic Problem", Quarterly Journal of Mechanics and Applied Mathematics, Vol. 27, Pt. 1, 1974, pp. 129-142.
42. Greenspan, D and Werner, P., "A Numerical Method for the Exterior Dirichlet Problem for the Reduced Wave Equation", Archives of Rational Mechanics and Analysis, Vol. 23, Pt. 4, 1966, pp. 288-316.

43. Gradshteyn, I. S. and Ryzhik, I. M., Table of Integrals, Series, and Products, Academic Press, New York, Sixth Printing, 1972.
44. Hitchcock, A. J. M., "Polynomial Approximations to Bessel Functions of Order Zero and One and to Related Functions", Mathematical Tables and Other Aids to Computations, Vol. 11, 1957, pp. 86-88.
45. Bisplinghoff, R. L., et al, Aeroelasticity, Addison-Wesley Publishing Company, Reading, MA, 1957.
46. Ward, R. C., "An Extension of the QZ Algorithm for Solving the Generalized Matrix Eigenvalue Problem", NASA TN D-7305, July 1973.
47. Schied, F., Numerical Analysis, Schaum's Outline Series, McGraw-Hill, New York, 1968, p. 318.
48. Bell, W. A., "An Integral Approach for Determining the Resonant Frequencies and Natural Modes of Arbitrarily Shaped Ducts", Research Initiation Proposal # P4K0667-000 submitted November 29, 1973, Georgia Institute of Technology, Atlanta, GA.
49. Bell, W. A., Meyer, W. L., and Zinn, B. T., "Prediction of the Acoustics of Solid Propellant Rocket Combustors by Integral Techniques", to be published in the Proceedings of the 12th JANNAF Meeting, Newport, RI, August 11-15, 1975.
50. Bell, W. A., Meyer, W. L., and Zinn, B. T., "An Integral Approach for Determining the Resonant Frequencies and Natural Modes of Arbitrarily Shaped Ducts", Proceedings of the 3rd Interagency Symposium on University Research in Transportation Noise, Salt Lake City, UT, November 12-14, 1975.
51. Bell, W. A., Meyer, W. L., and Zinn, B. T., "Predicting the Acoustic Properties of Arbitrarily Shaped Bodies by Use of an Integral Approach", AIAA Paper No. 76-494, to be presented at the 3rd AIAA Aero-Acoustics Meeting, July 20, 1976.